Libya, geographically located in North Africa, is characterised by vast stretches of desert, with the Sahara Desert dominating much of its landscape. The country has large hydrocarbon reserves, which make a significant contribution to its economy and to global oil production. Agriculture in Libya faces challenges due to the arid climate, the scarcity of water resources and the small amount of arable land. The sector is heavily dependent on irrigation. Climate change is producing a significant rise in temperatures and changes in rainfall patterns, which are having an increasing impact on agriculture, water resources and the environment in general.

This first study addresses all these issues to show the potential of Earth observation data, and in particular the free data from the Sentinel satellites of the European Copernicus programme.

Figure 1a shows the administrative division of Libya, delineating its various governorates (*muhafazat*) as well as its Economic Exclusion Zone (EEZ). Figure 1b shows the Copernicus Digital Elevation Model (DEM), which illustrates Libya's mainly desert plains and scattered mountainous regions, highlighting its arid landscape.

Libya seen from space

Sentinel-3 OLCI, LU/LC, DEM

2D_layer_stack

Figure 2a shows the observations made on 12 August 2021 by the two satellites Sentinel-3A (left track) and Sentinel-3B (right track) equipped with the OLCI medium-resolution optical instrument.

Figure 2b shows one of the land use maps (LU/LC) produced periodically by the Copernicus C3S service. The classes shown in the legend were calculated mainly from Sentinel-3 OLCI data.

Fig.1: Governorates of Libya (a) and Digital Elevation Model (b).

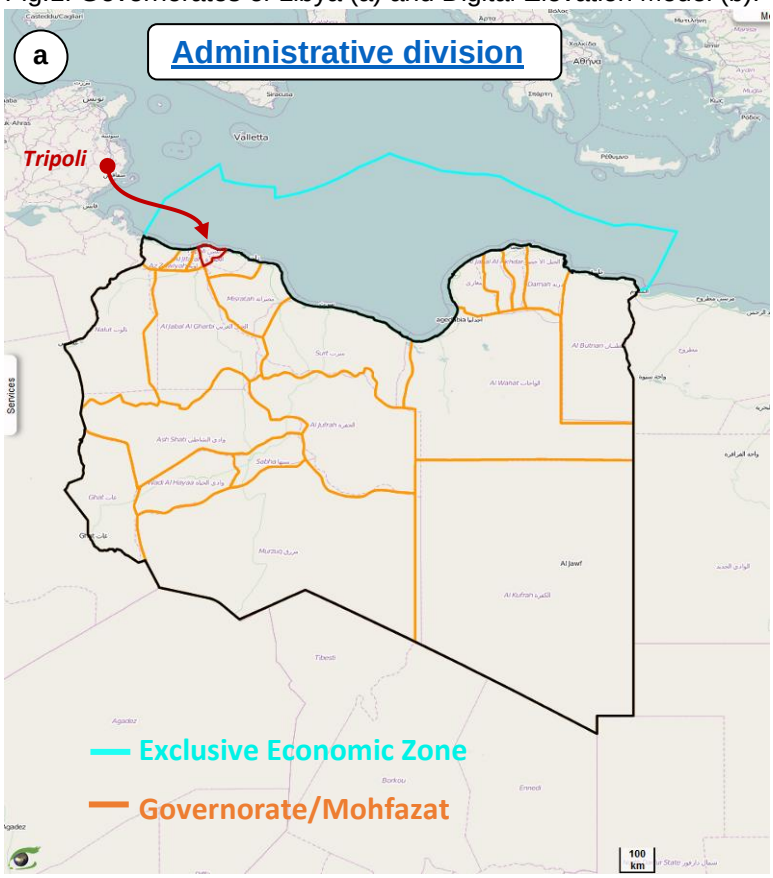

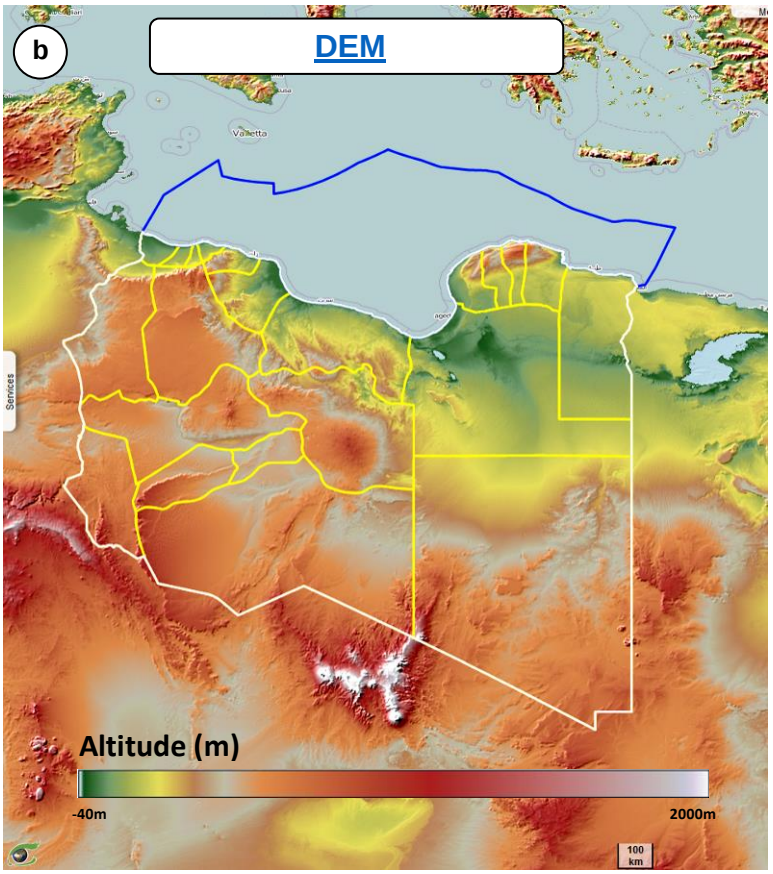

Fig.2: Sentinel-3 optical (a) and Copernicus land use / land cover (b).

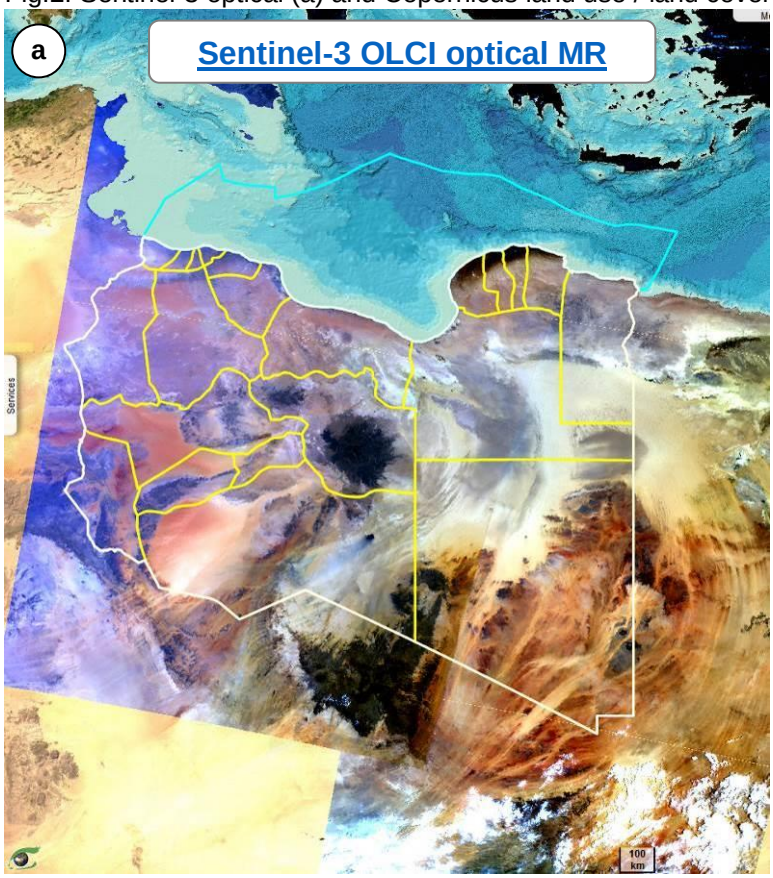

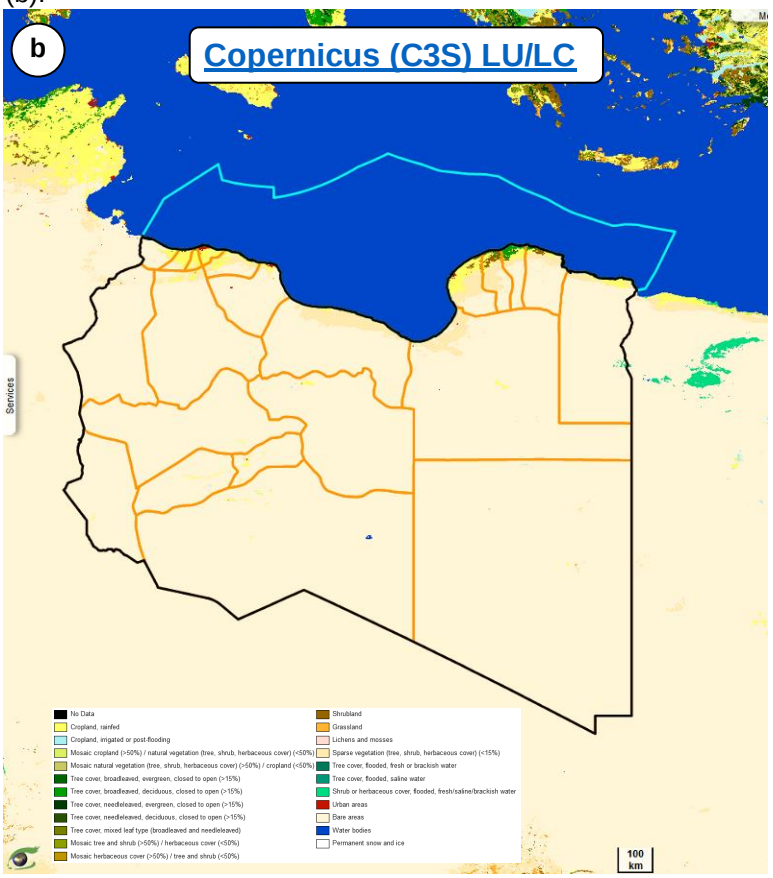

The Great Man-Made River (GMMR) project in Libya, a vast network of pipelines and infrastructure, aims to alleviate water scarcity by transporting water from the Nubian Sandstone Aquifer System across the desert. It serves as a crucial solution to provide freshwater resources for agricultural, industrial, and domestic needs in the country. Despite its scale and contribution to socio-economic development, challenges related to maintenance, sustainability, and environmental impact underline the necessity for ongoing management to ensure a reliable water supply and its long-term viability for Libya's future (Wikipedia).

The Great Man-Made River system plays a pivotal role in sustaining agriculture by providing a vital water supply to arid and semi-arid regions, promoting agricultural productivity and supporting crop cultivation.

Fig.3 illustrates a schematic view of the project and its different phases.

Fig.4a and Fig.4b show irrigated crops near east Jabal Hasouna well field and a zoom over Sarir pipe production plant respectively.

Water resources

Great Man-Made River project

Fig.3: Schematic drawing of the project “Great Man-Made River”. 2D_view

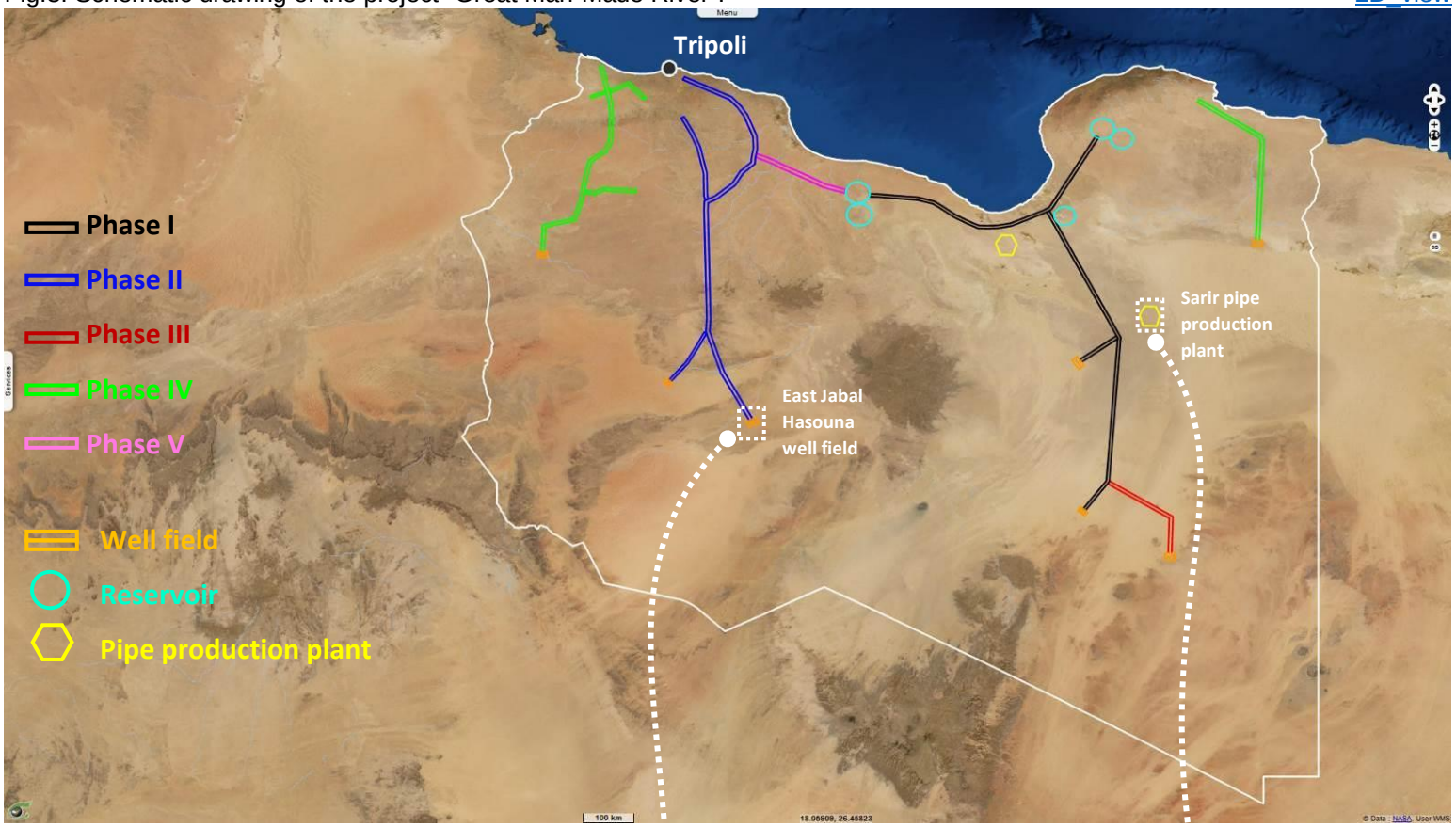

Fig.4: Irrigated crops near east Jabal Hasouna well field (a) and Sarir pipe production plant (b). left_view right_view

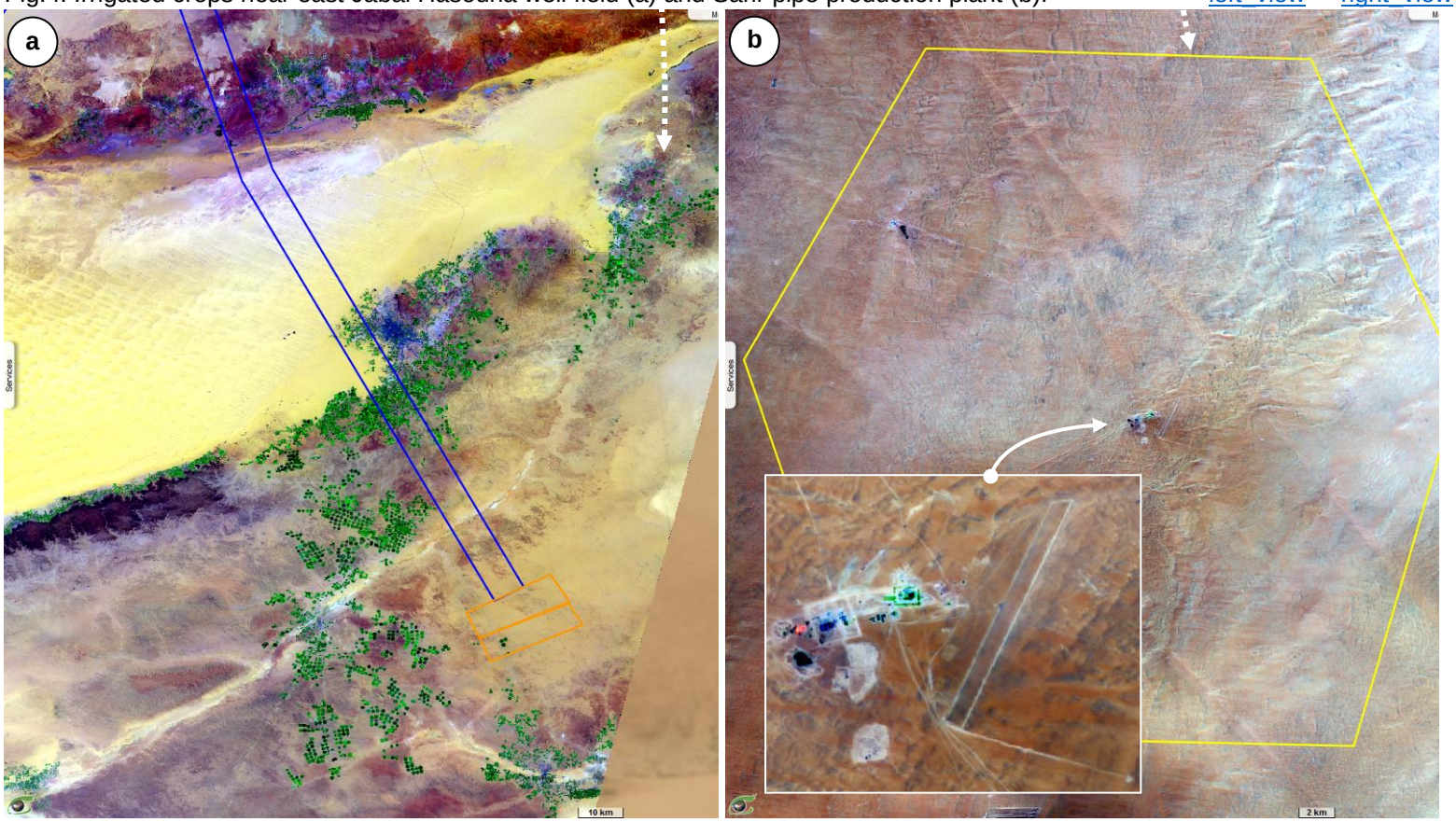

powered by AfEOS and VisioTerra

The Great Man-Made River Project has significantly modified the agricultural landscape of Libya's desert regions. By channelling water from the depths of the Sahara to these arid areas, it has opened the door to previously inconceivable irrigated agriculture. This regular irrigation has transformed these barren lands into fertile fields, allowing for the cultivation of cereals, vegetables, and fruits. This initiative has substantially increased food production in previously hostile Libyan regions. The Great Man-Made River Project represents a critical resource in response to the challenges of climate change, particularly among the observed decrease in precipitation these last years.

Fig.5a and Fig.5b show two Sentinel-2 optical images acquired on 2018 and 2023 during the same period (April month) respectively. The figures display various forms of pivot irrigation-based farming.

Fig.6a shows the difference of the Normalised Difference Vegetation Index (NDVI) between 2023 and 2018. In this figure, we observe a proliferation of agricultural parcels while an analysis indicating a drastic decline in precipitation between 2018 and 2023 as given by Fig.6b. Fig.6c shows the mean precipitation over the wet season (September to February) confirming this decline. The results demonstrate that the artificial river ensures essential water supply for agriculture in regions affected by this declining precipitation, consequently providing resilience against climate variations.

Water resources

Crops irrigation

Fig.5: Sentinel-2 optical images acquired on 2018 and 2023 during the same period. animation

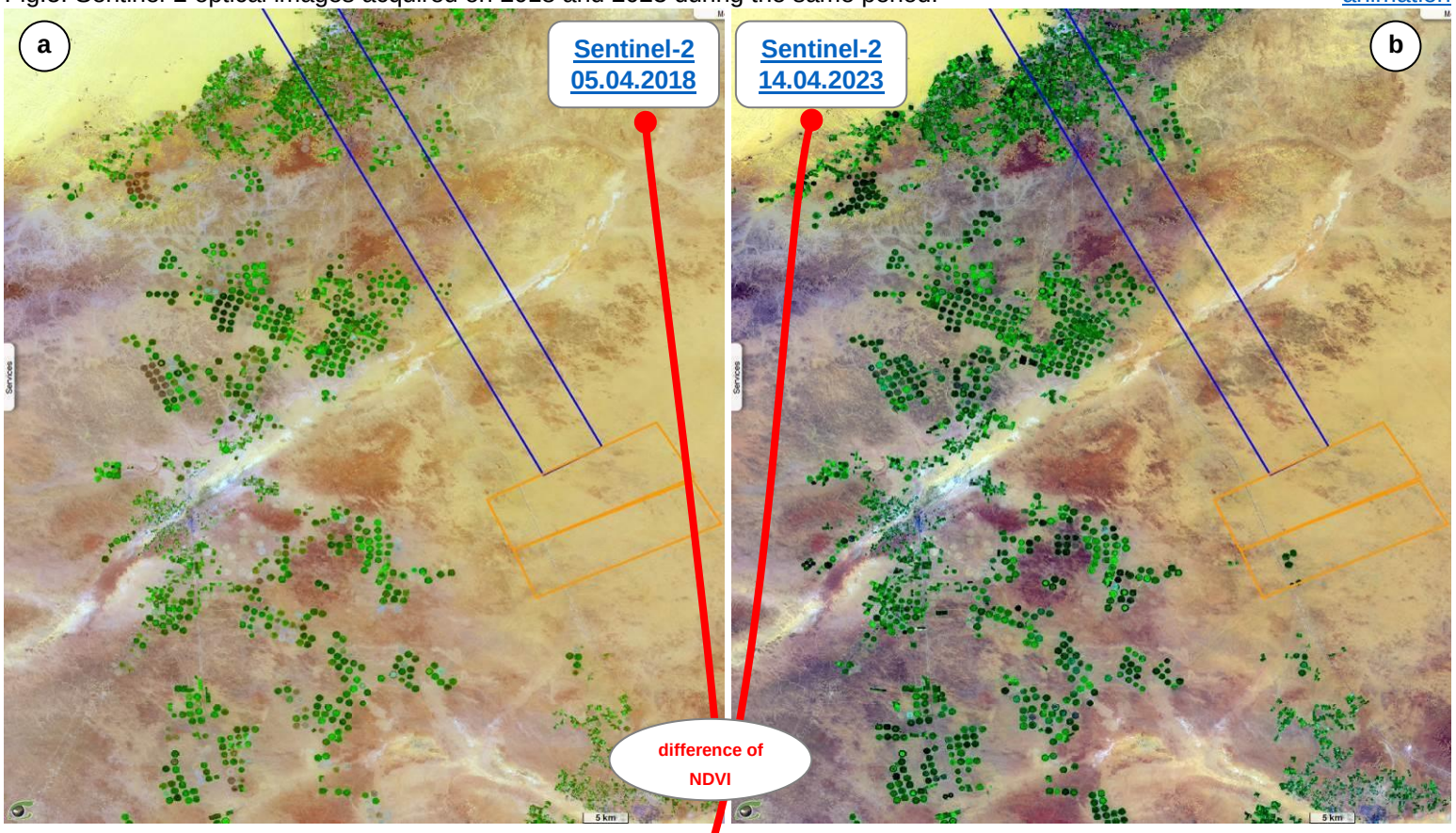

Fig.6: Difference of the NDVI between 2023 and 2018 (a), monthly precipitations (b) and precipitation during the wet season (c).

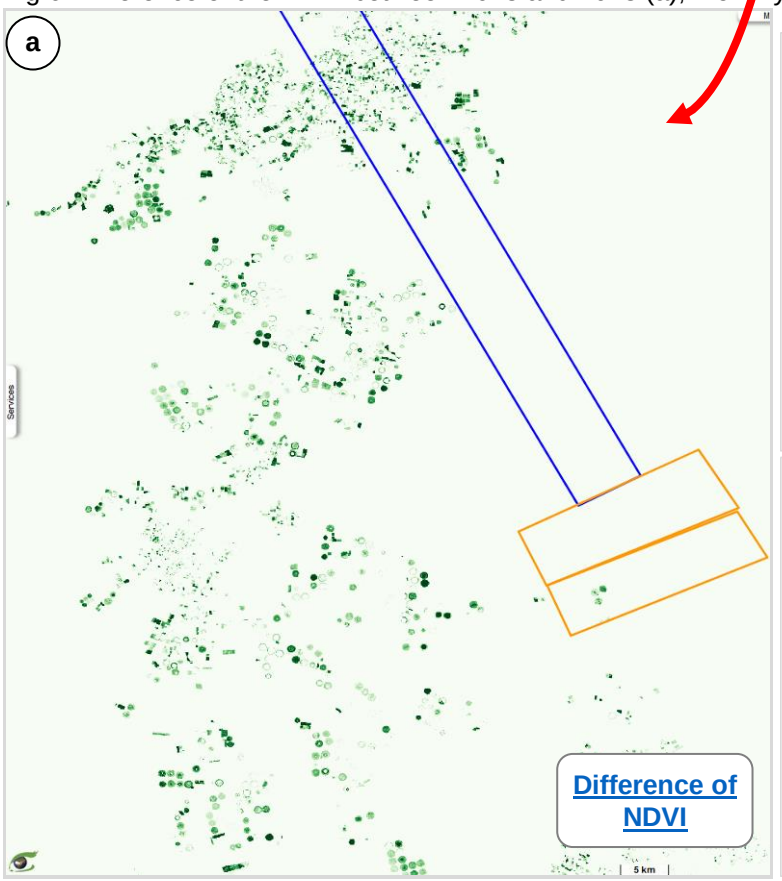

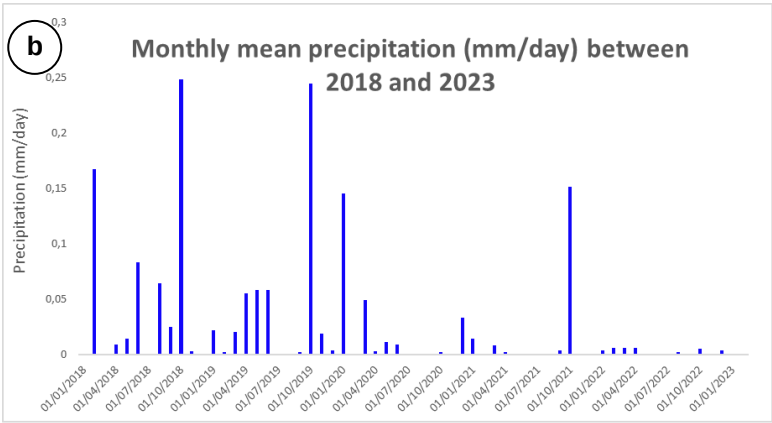

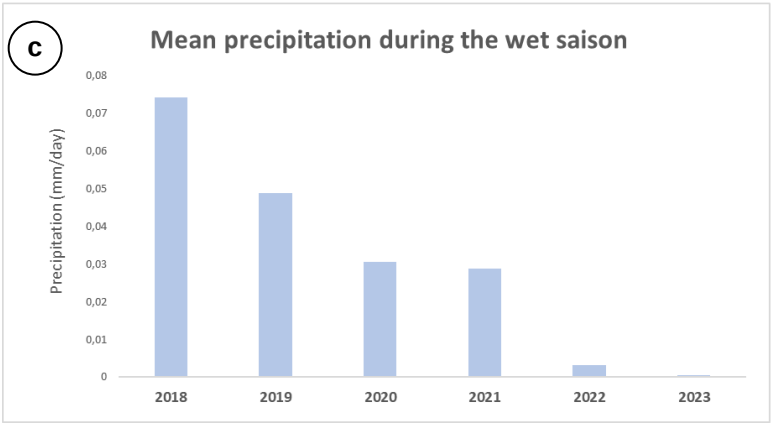

Agriculture monitoring (1a)

Irrigated cereal parcel (Wadi al Hayat governorate)

This section shows a cereal parcel, captured through Very High Resolution (VHR) image (Fig.7a) and Sentinel-2 High Resolution (HR) image (Fig.7b). The figures display a distinctive pattern of pivot irrigation. The efficiency of pivot irrigation lies in its ability to minimize water wastage. The circular layout of fields is characteristic of this system. This precise and targeted approach aids in rational water management, promoting optimal crop growth while conserving water resources.

Fig.8a and Fig.8b show the vegetation indicator (NDVI) and the soil moisture indicator (NDWI-SM) respectively computed from the Sentinel-2 scene observed on 14.04.2023.

The NDVI is among the most commonly used indicators to monitor the percentage of vegetation cover in an area.

The NDWI-SM (Normalised Difference Water Index - Soil Moisture) was developed by Gao (1996) and measures the liquid water contained in the vegetation cover.

$$NDVI = \frac{NIR - R}{NIR + R} \quad , \quad NDWI - SM = \frac{NIR - SWIR}{NIR + SWIR}$$

Where NIR is the near infrared (band 8), SWIR is the mid-infrared band (band 11) and R is the red band (band 4). The bands are those of the Sentinel-2 MSI optical sensor.

Fig.7: VHR (a) and Sentinel-2 (b) views of agricultural parcel. left_view right_view

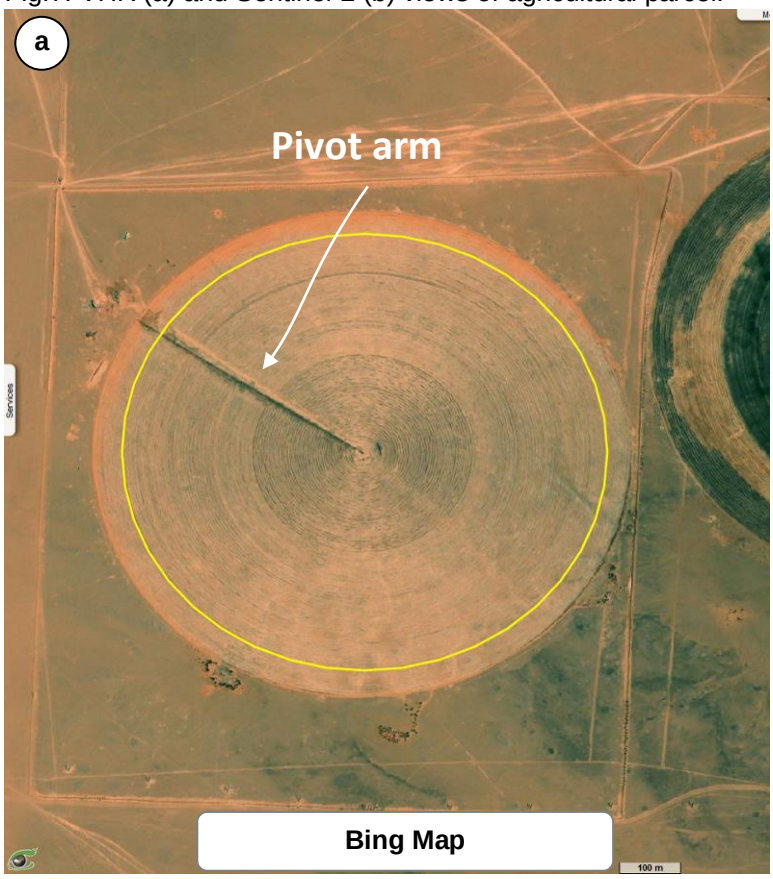

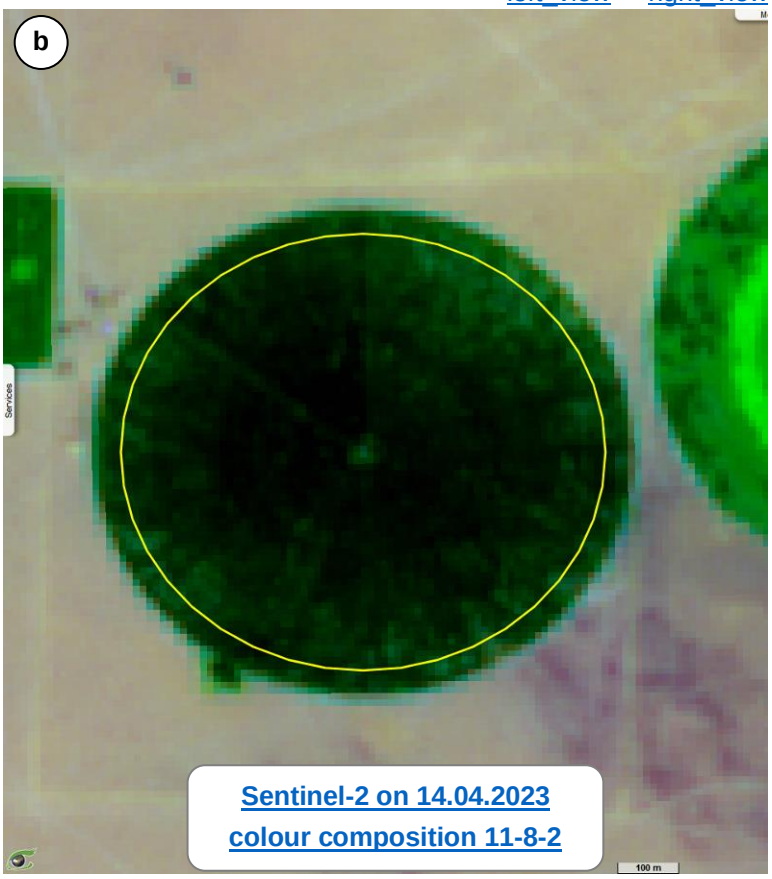

Fig.8: Vegetation index (a) and soil moisture index (b). left_view right_view

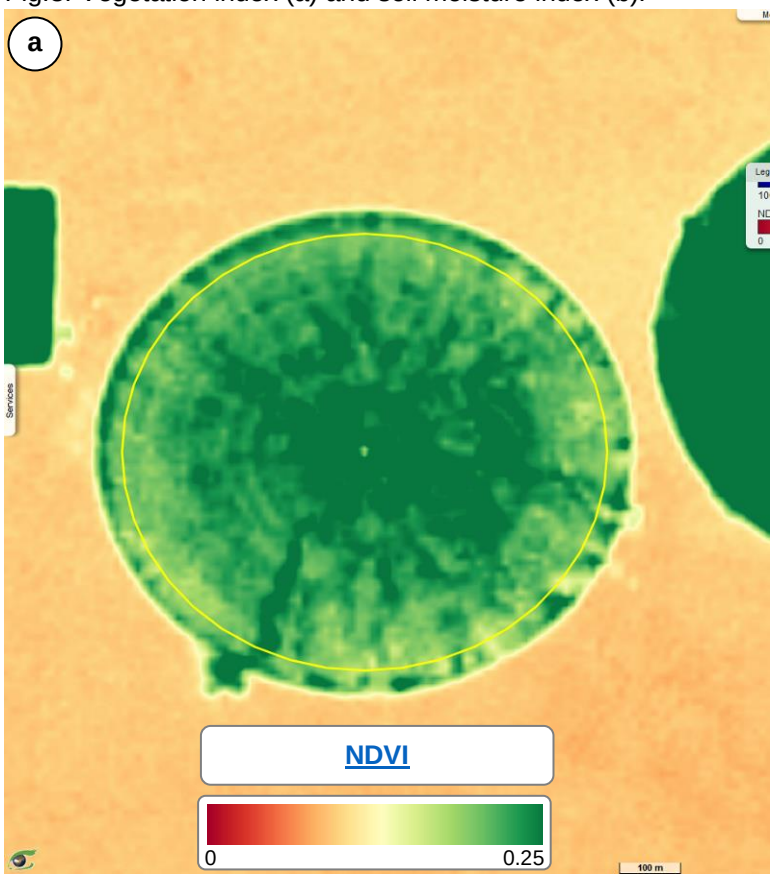

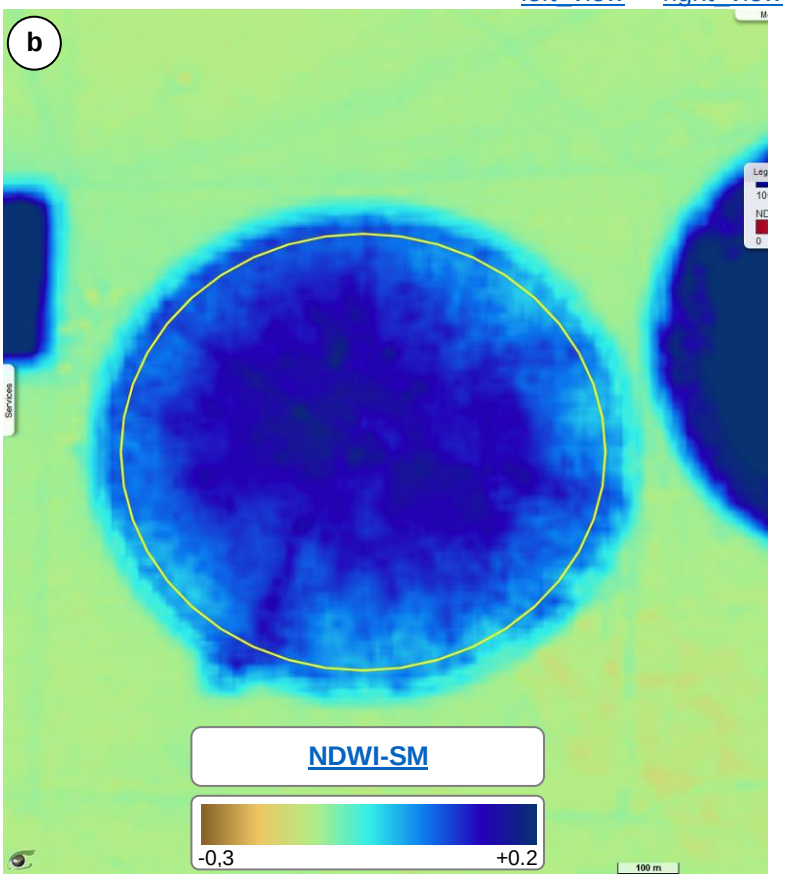

Fig.9 shows Copernicus ERA5-Land monthly precipitations over the parcel of pivot irrigation from 2018 to 2023 in chronological (Fig.9a) and seasonal (Fig.9b) views. One may notice that the precipitations are very low (less than 0.2 mm of water per day averaged over each month) and that seasons are not clearly observed.

Fig.10 shows the mean of Sentinel-2 NDWI-SM on the area of interest from 2018 to 2023 in chronological (Fig.10a) and seasonal (Fig.10b) views.

Fig.11 shows the mean of Sentinel-2 NDVI on the area of interest from 2018 to 2023 in chronological (Fig.11a) and seasonal (Fig.11b) views.

The NDVI correlate well with the soil moisture computed along time by Sentinel-2 during from 2018 to 2023. The soil moisture and the vegetation growth are maximal during February-March period.

The NDWI-SM does not correlate well with precipitations confirming that the parcel is not rainfed.

All the statistics are computed on the parcel only.

Agriculture monitoring (1b)

Irrigated cereals
Time series analysis

Fig.9: Time series of precipitations from 2018 to 2023 on the plot in chronological (a) and seasonal (b) views.

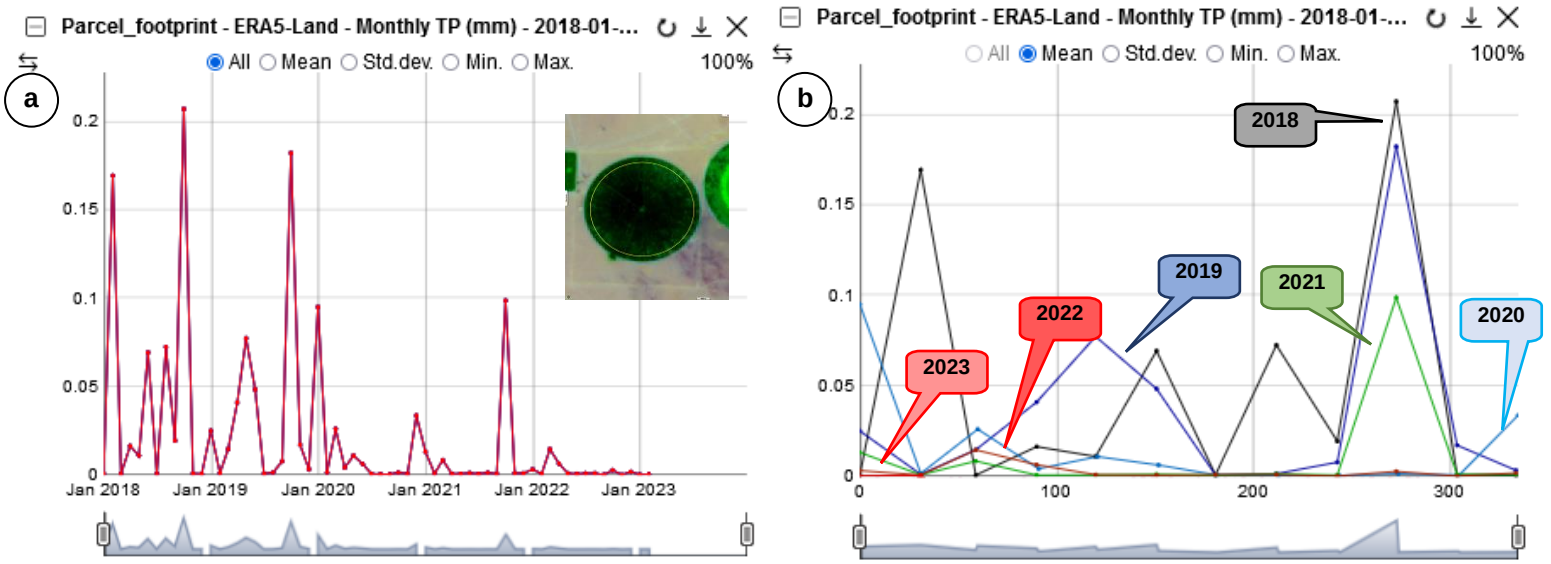

Fig.10: Time series from 2018 to 2023 of Soil Moisture (NDWI-SM) Index in chronological (a) and seasonal (b) views.

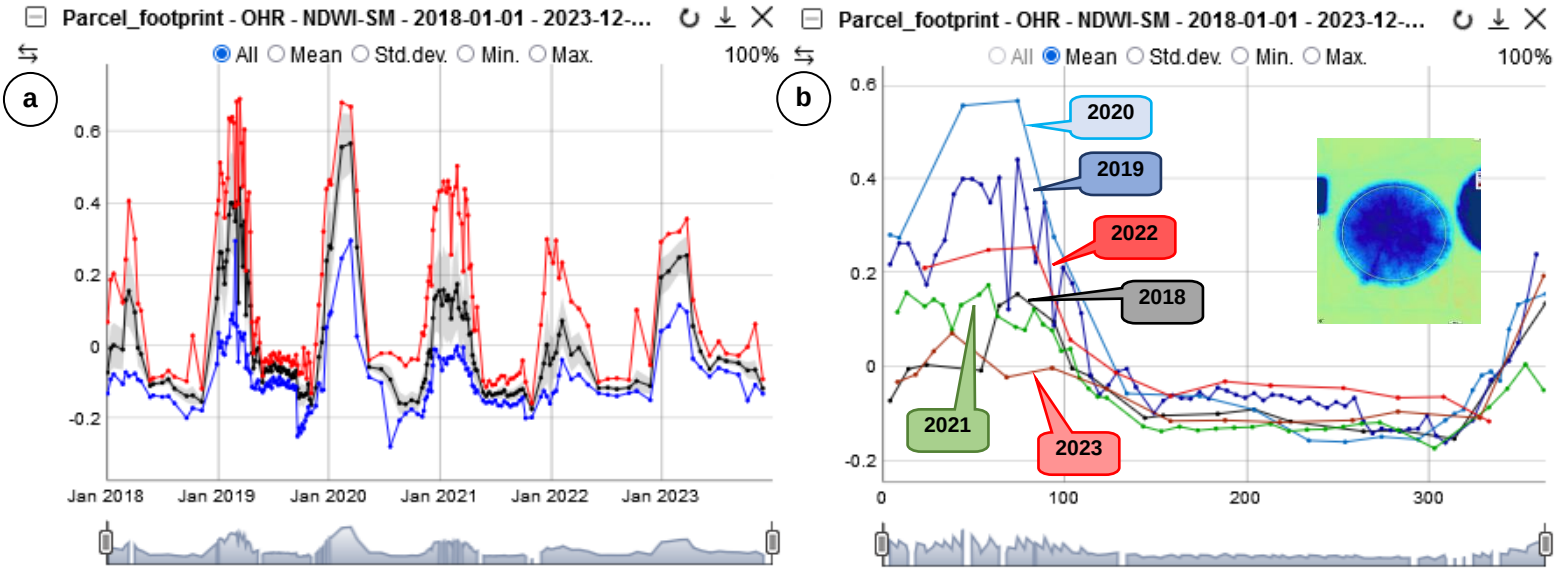

Fig.11: Time series from 2018 to 2023 of NDVI in chronological (a) and seasonal (b) views.

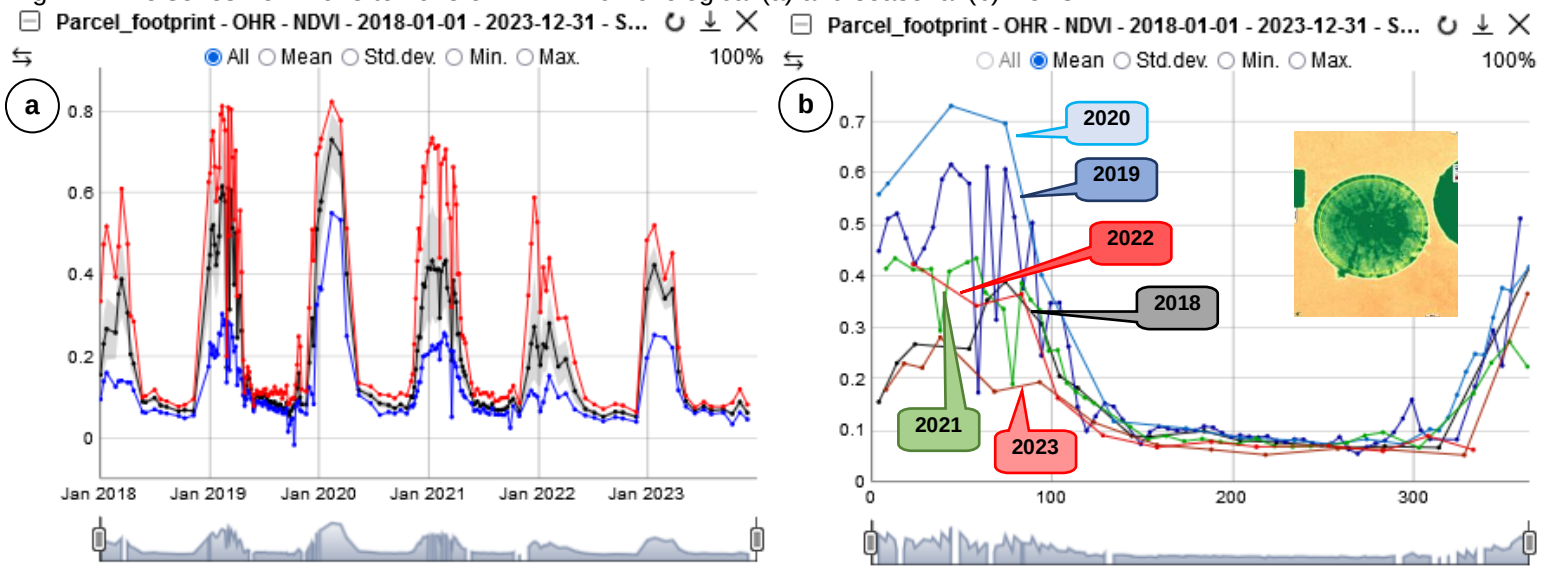

powered by AfEOS and VisioTerra

This example showcases a citrus plot located in northern Libya (south of Tripoli). Figure 12a displays a very high-resolution image while Figure 12b showcases a Sentinel-2 image, both centred on the plot. Figures 13a and 13b respectively present the Soil Adjusted Vegetation Index (SAVI) and the NDWI-SM.

The SAVI (Soil Adjusted Vegetation Index) is a vegetation indicator developed as a modification of the NDVI to correct for the influence of soil response when vegetation coverage is low.

$$SAVI = \frac{NIR - R}{NIR + R + L} \times (1 + L)$$

"L" is a correction factor ranging from 0 for very high vegetation cover to 1 for very low vegetation cover. The most commonly used value is 0.5, corresponding to intermediate vegetation cover. Like the NDVI (Normalised Difference Vegetation Index), the SAVI goes from negative or null values (no-vegetation) to +1 value (vegetated area up to the saturation).

Fig.13a and Fig.13b show that, as for the cereal plot (see Fig.8a and Fig.8b), the vegetation indicators (here SAVI) and surface humidity (NDWI-SM) are correlated.

Agriculture monitoring (2a)

Rainfed citrus parcel (Tripoli governorate)

Fig.12: Citrus plot (Tripoli) viewed through Bing (a) and Sentinel-2 (28.01.2020, b). left_view right_view

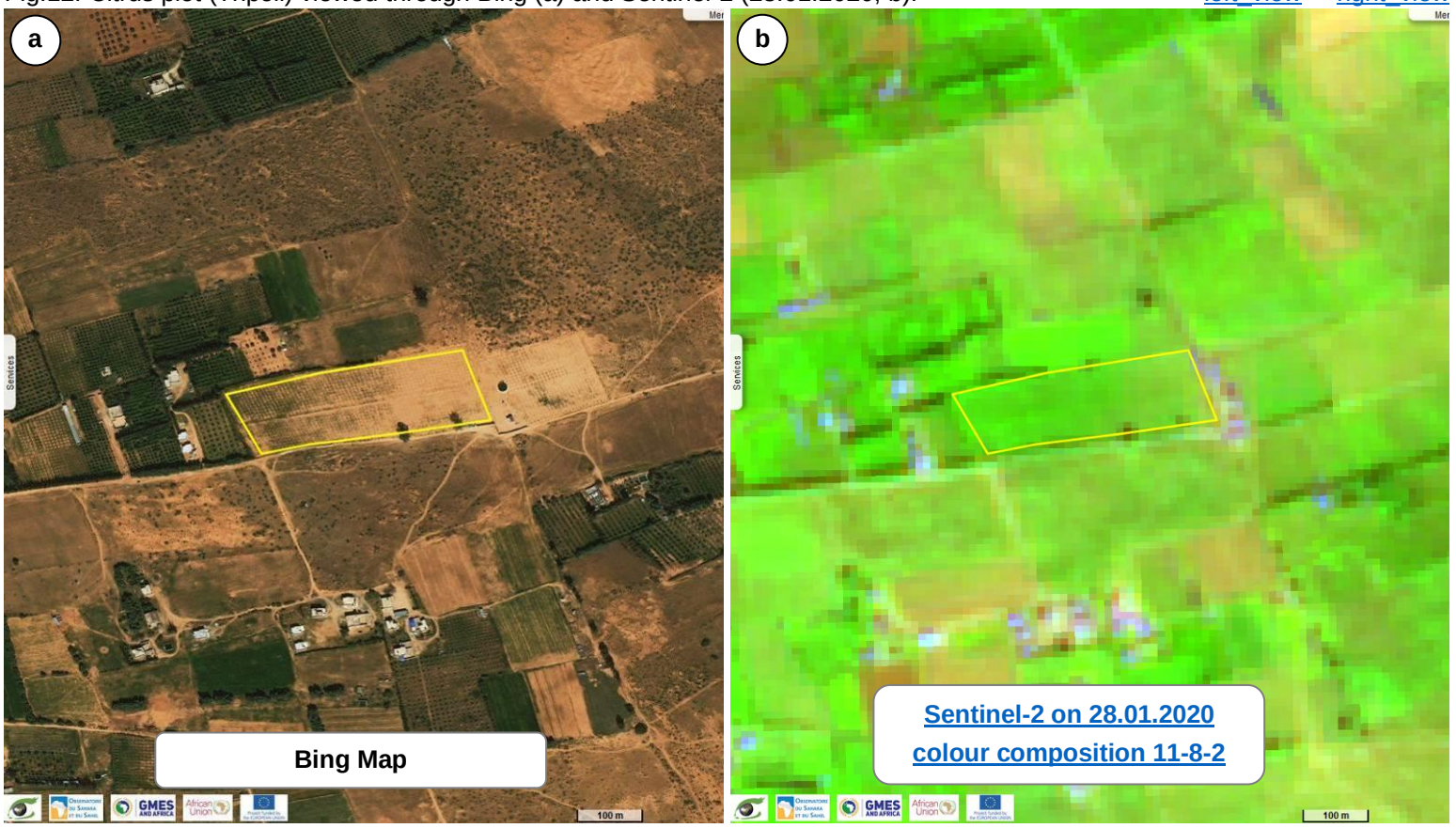

Fig.13: Vegetation (a) and soil moisture (b) indices. left_view right_view

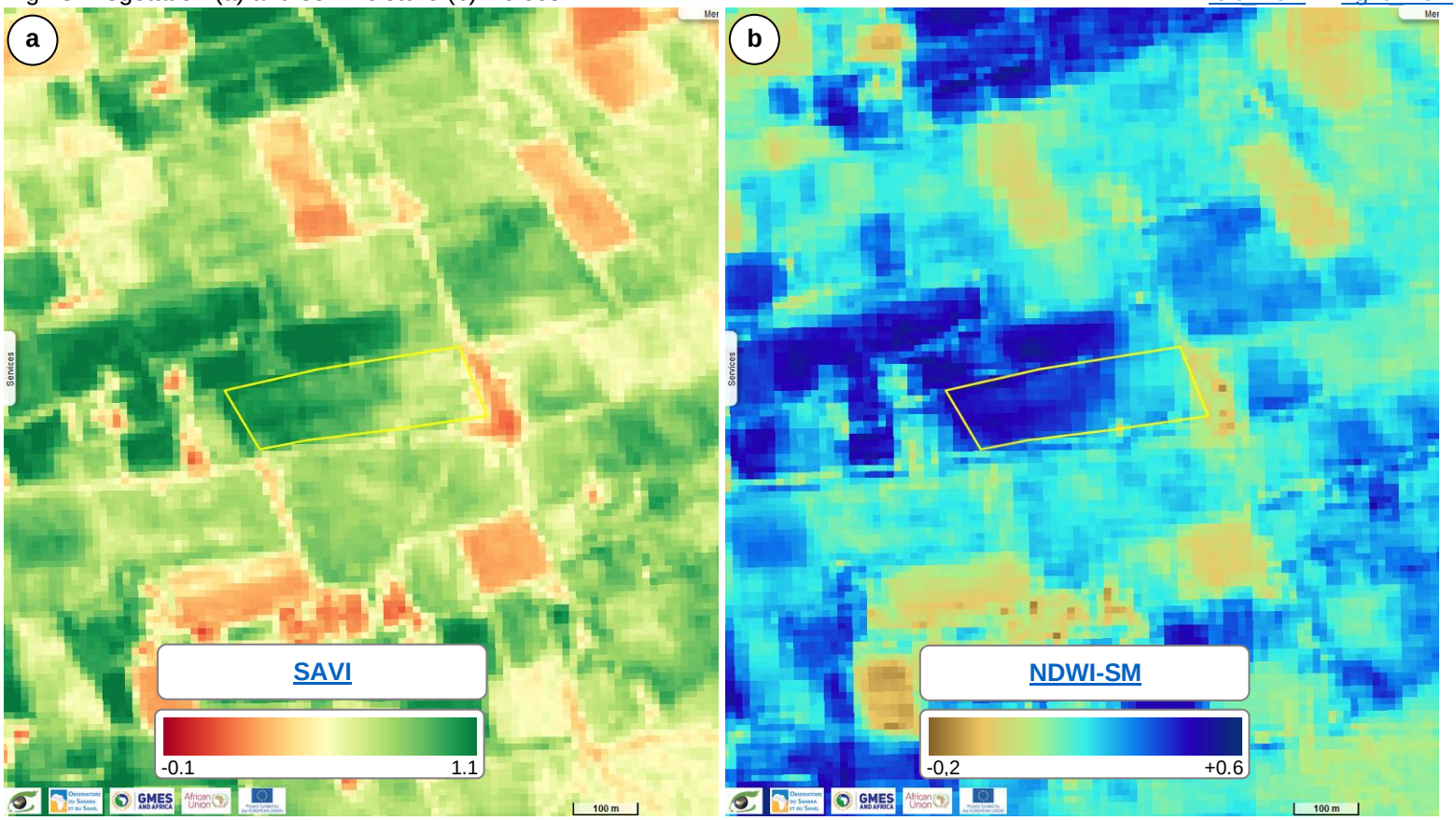

Agriculture monitoring (2b)

Rainfed citrus parcel
Time series analysis

Figures of this page show a multitemporal analysis performed over three years from 2018 to 2020.

Compared with the precipitations observed on Wadi al Hayat governorate (see Fig.9), averaged daily precipitations on the Tripoli region are much higher (around 200 mm / day) during the wet season (Fig.14). Furthermore, dry and wet seasons are clearly distinguishable.

For this citrus crop plot example, precipitations (Fig.14), soil moisture (Fig.15), and vegetation index (fig.16) all exhibit strong correlation. This correlation is a strong indicator of rainfed cultivation. Another presumption of rainfed cultivation is given by the analysis of the rainfall peak (Fig.14a) that precedes the maxima of soil moisture (Fig.15a) and vegetation (Fig.16a) indices.

The vegetation index is compliant with the phenological cycle of citrus, displaying a growth phase starting in August and a harvesting period between March and April. The consistent behaviour of this vegetation indicator over the three years may suggest roughly comparable yields.

All the statistics along the time (Fig.10a, 11a, 15a, 16a) show the minimum, maximum, mean and standard deviation of the indicator values in the plot. One may note that measurements in the citrus field are much more dispersed than those in the pivot crop. These inhomogeneities can help the farmer to adapt the layout of the trees, soil digging, watering, organic amendments… according to these observations.

Fig.14: Time series data from 2018 to 2020 illustrating precipitation on the plot in chronological (a) and seasonal (b) views.

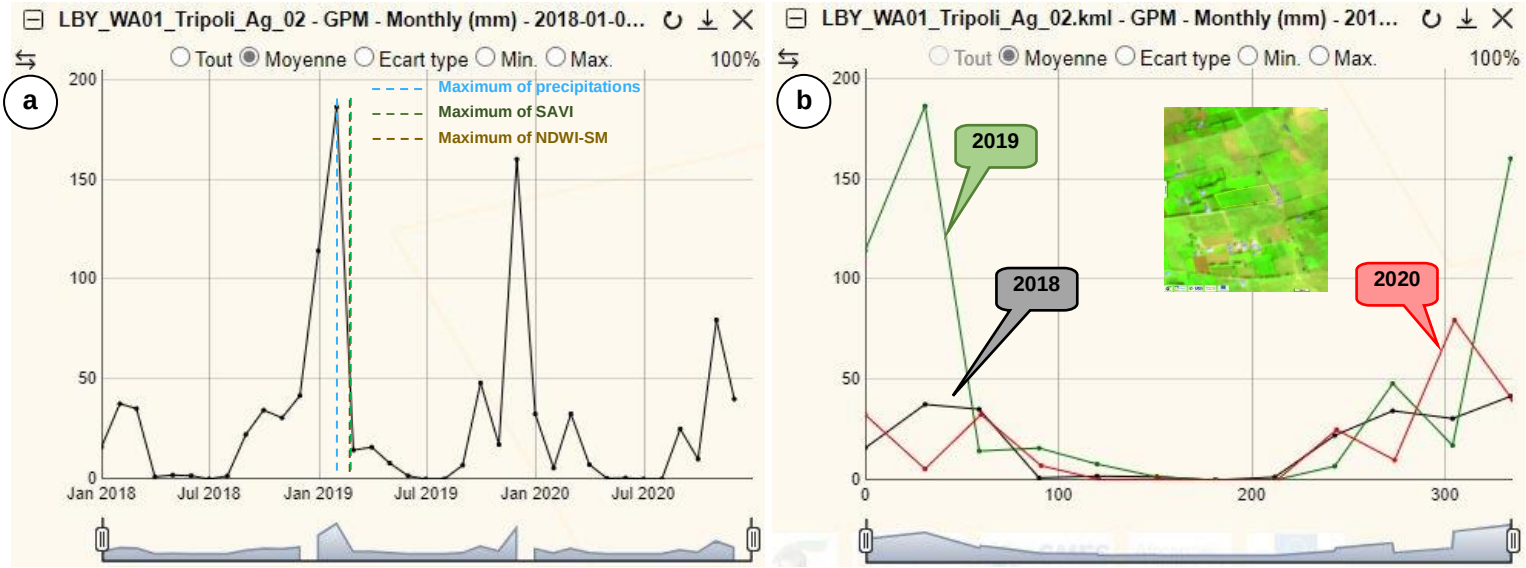

Fig.15: Time series from 2018 to 2020 of Soil Moisture (NDWI-SM) Index in chronological (a) and seasonal (b) views.

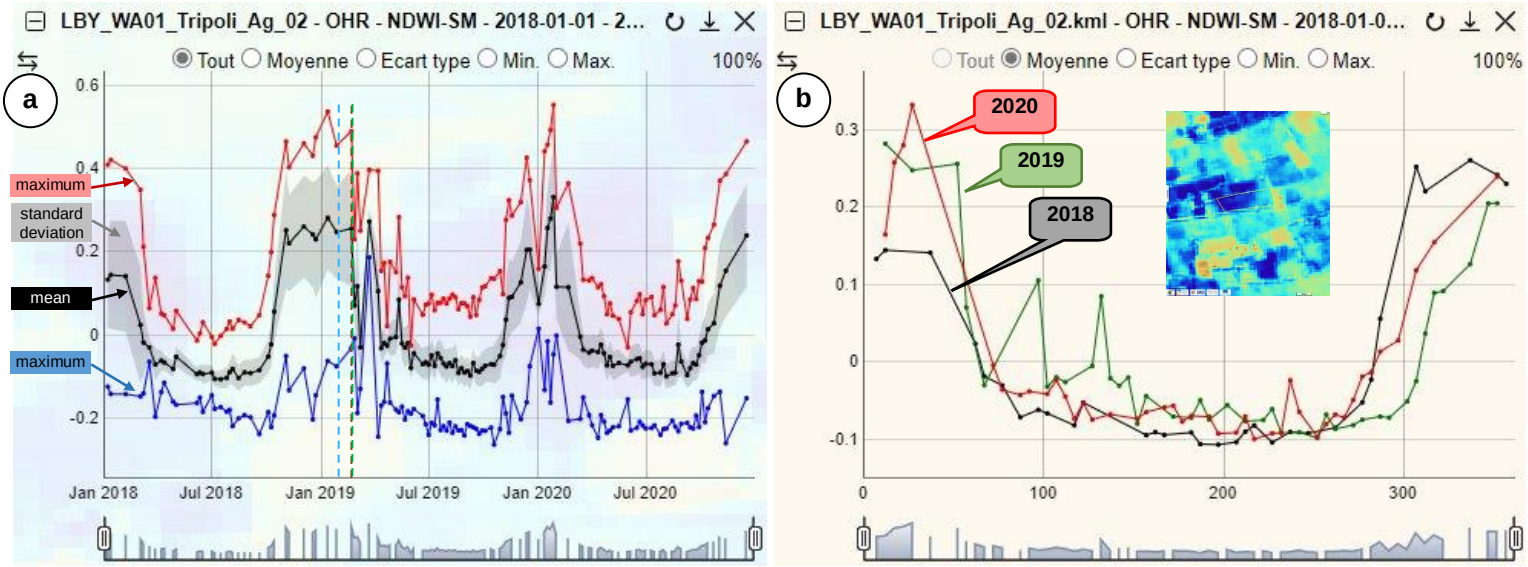

Fig.16: Time series from 2018 to 2023 of SAVI in chronological (a) and seasonal (b) views.

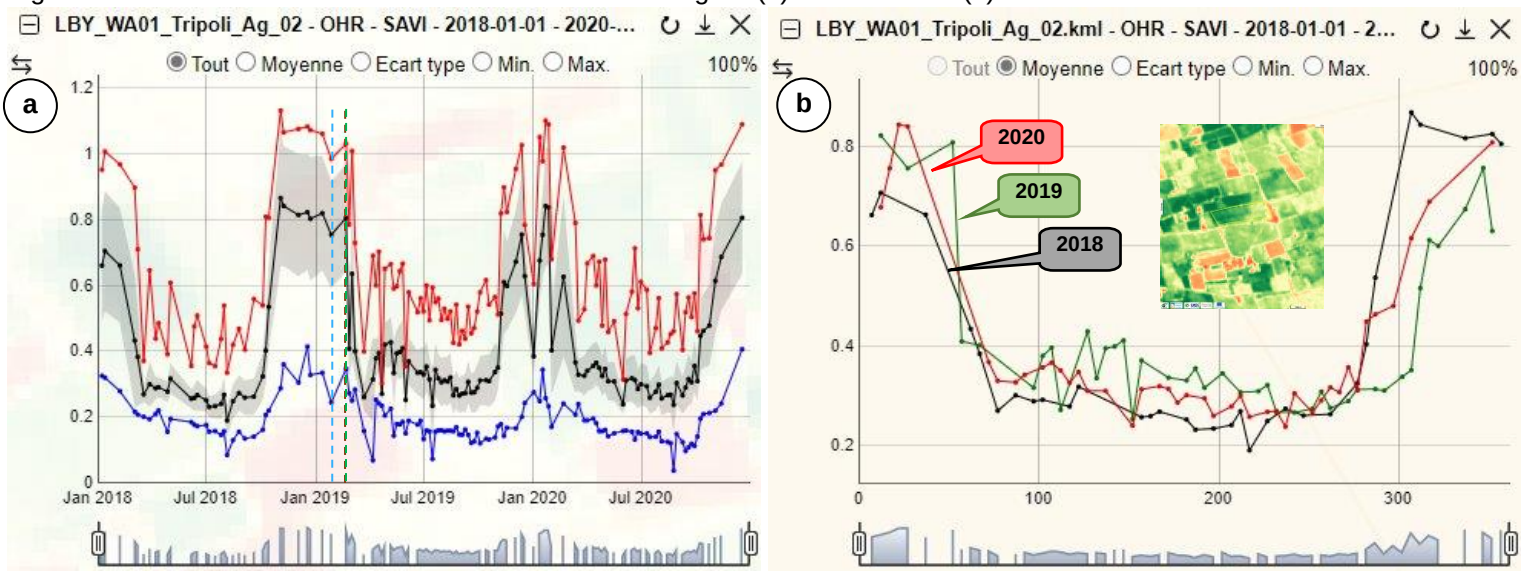

Drougths monitoring

Underground water resources issues

In Libya, prolonged drought has led to a significant decline in groundwater levels, resulting in the gradual drying of once-thriving oases. The increased demand for water, amplified by agricultural needs and the ambitious Great Man-Made River project, has put under pressure the region's aquifers. As these vital underground reservoirs diminish, some are succumbing to the severe impacts of diminished underground water resources.

Fig.17 show the decreasing of water in Ibn Aati oasis (Wadi al Hayat governorate) observed on Sentinel-2 images between 2015 and 2022. This decreasing is confirmed by the open water indicator (Fig.8)

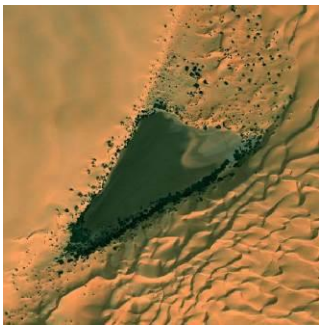

Fig.17: Decreasing of water in Ibn Aati oasis observed on Sentinel-2 images between 2015 and 2022. animation

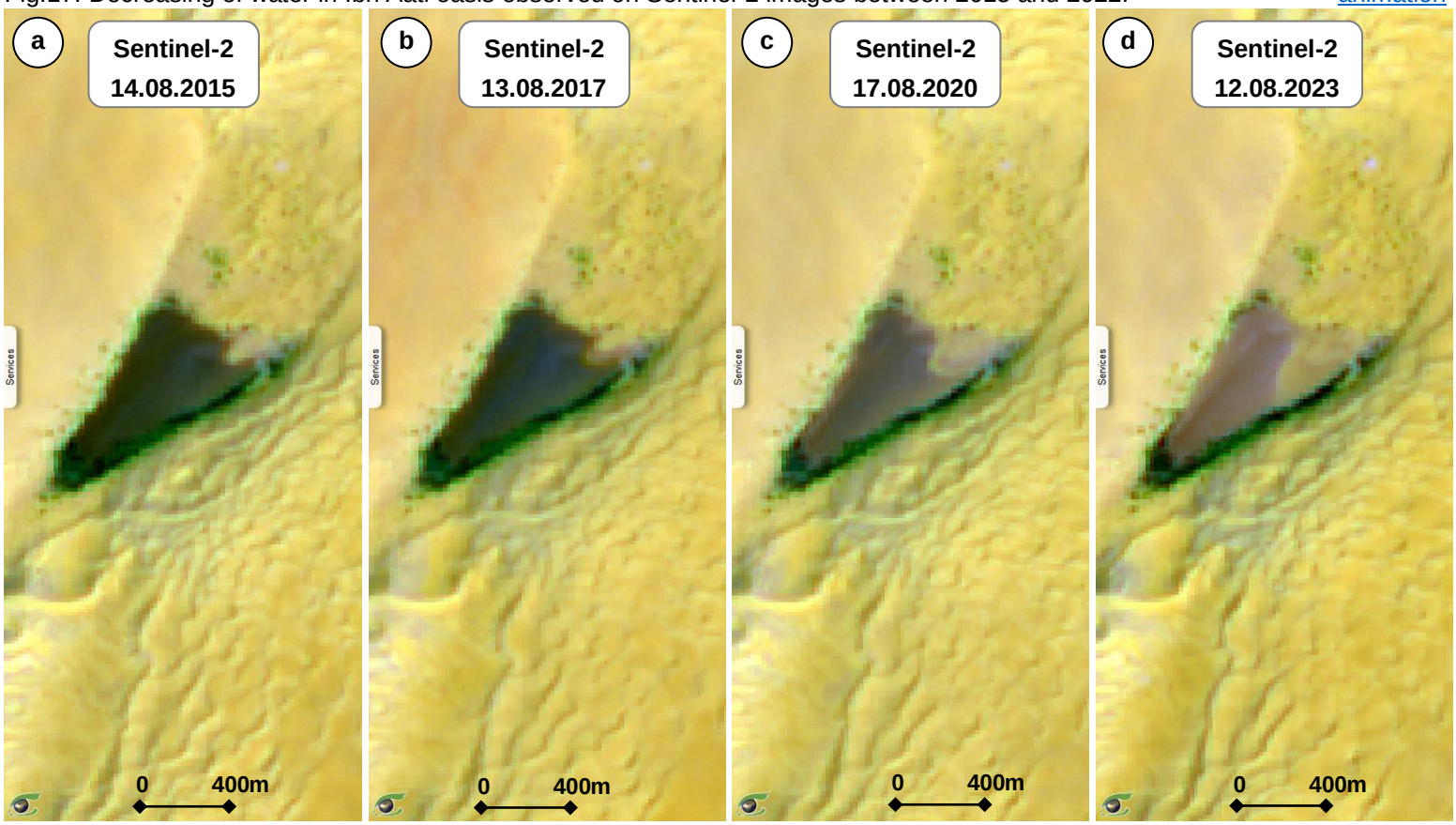

Fig.18: NDWI-OW index over Ibn Aati oasis between 2015 and 2022. animation

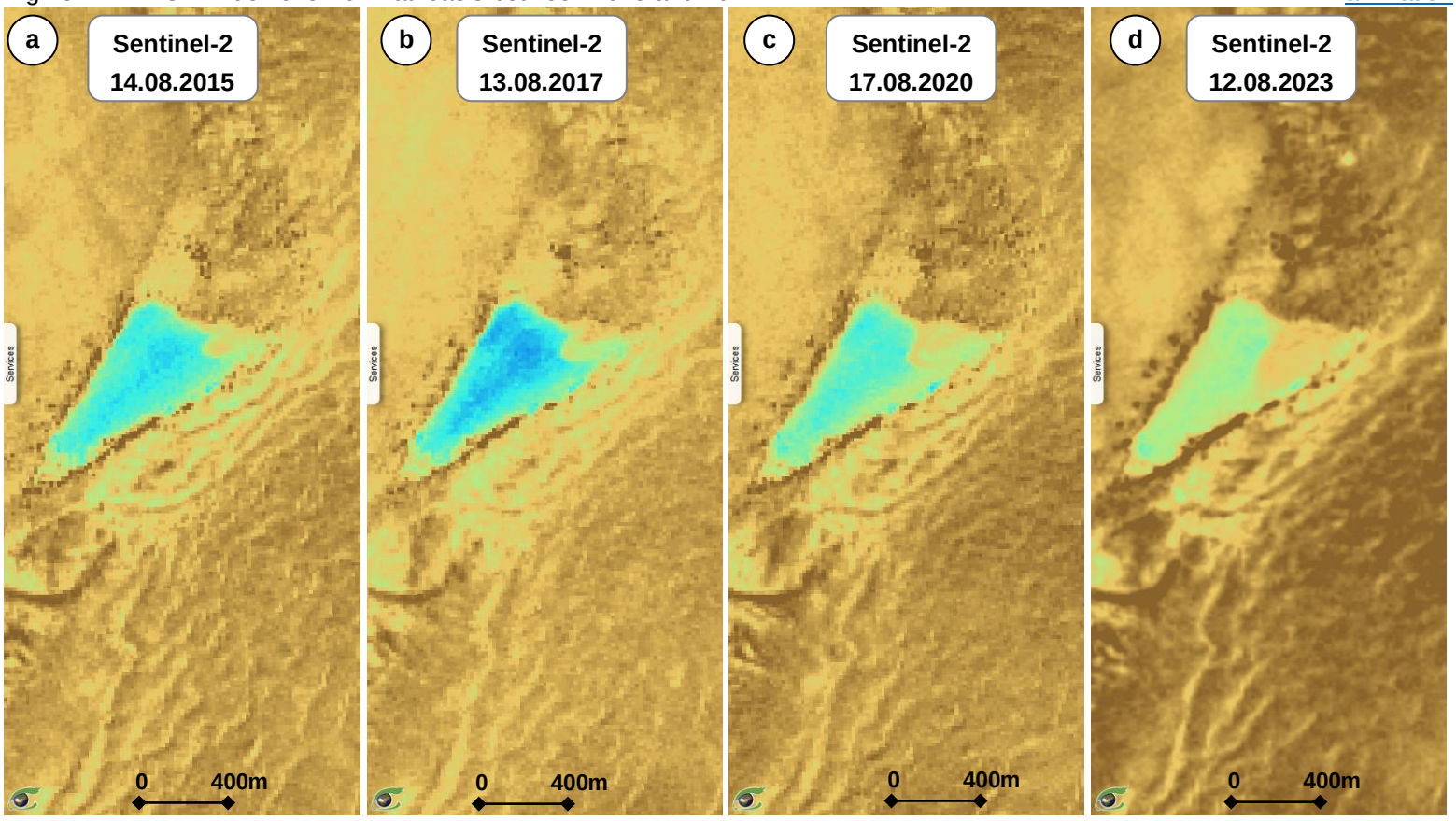

Beyond the challenges posed by drought, Libya faces others issues such as urban expansion and population growth.

Fig.19 shows Sentinel-2 optical observed on 25 August 2023 (Fig.19a) and the mean of six (6) Sentinel-1 radar scenes observed from 2nd December 2023 to 12 February 2023 (Fig.19b). This colour composition maps the mean of VV polarisation, VH polarisation and the variation coefficient of VH on red, green and blue planes respectively.

Fig.20 shows the Land-Use / Land-Cover (LU/LC) models produced by the Copernicus Climate Change Service (C3S) for years 2000, 2010 and 2020.

Fig.21 shows the population density model called Global Human Settlement (GHS) produced by the Joint Research Centre (JRC) for the same years 2000, 2010 and 2020.

The figures provide a clear insight into urban evolution over time. Sequential views of land cover across multiple dates demonstrate significant urban expansion.

The "animation" hyperlooks open a window that lets you "launch" cyclical views of the images.

Urbanisation & population monitoring

Tripoli

Fig.19: Sentinel-2 optical agriculture (a) and Sentinel-1 radar as a mean of 6 scenes: 02.12.2023 → 12.02.2024 - Views of Tripoli.

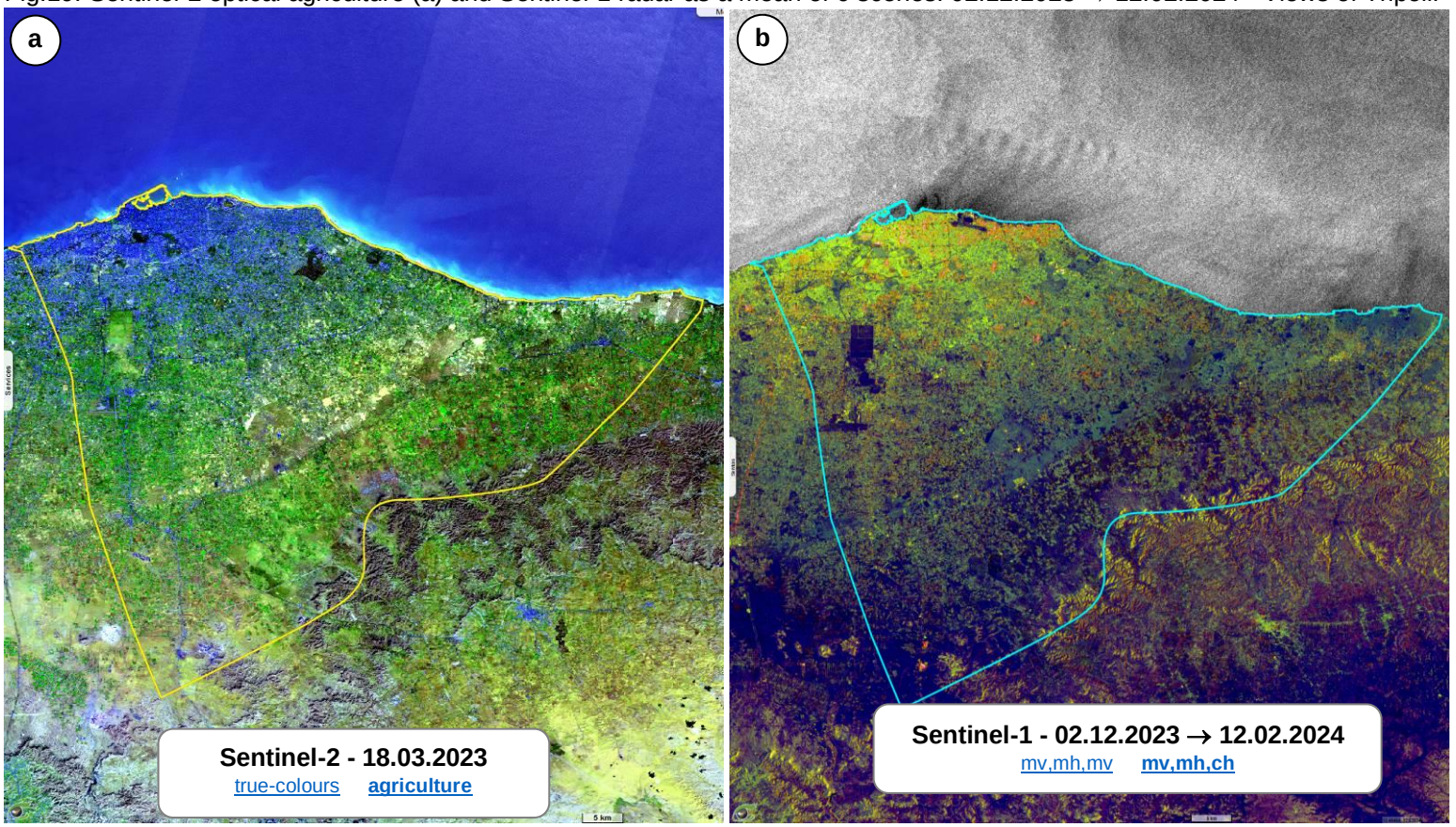

Fig.20: Land use /land cover over Tripoli in 2000 (a), 2010 (b) and 2020 (c). animation

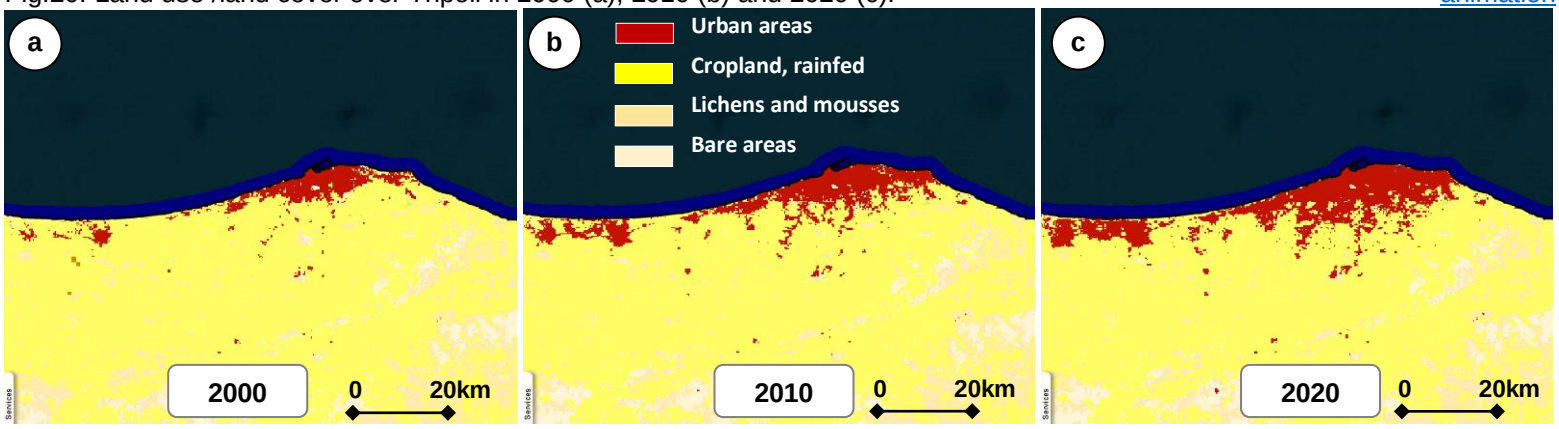

Fig.21: Population over Tripoli in 2000 (a), 2010 (b) and 2020 (c). animation

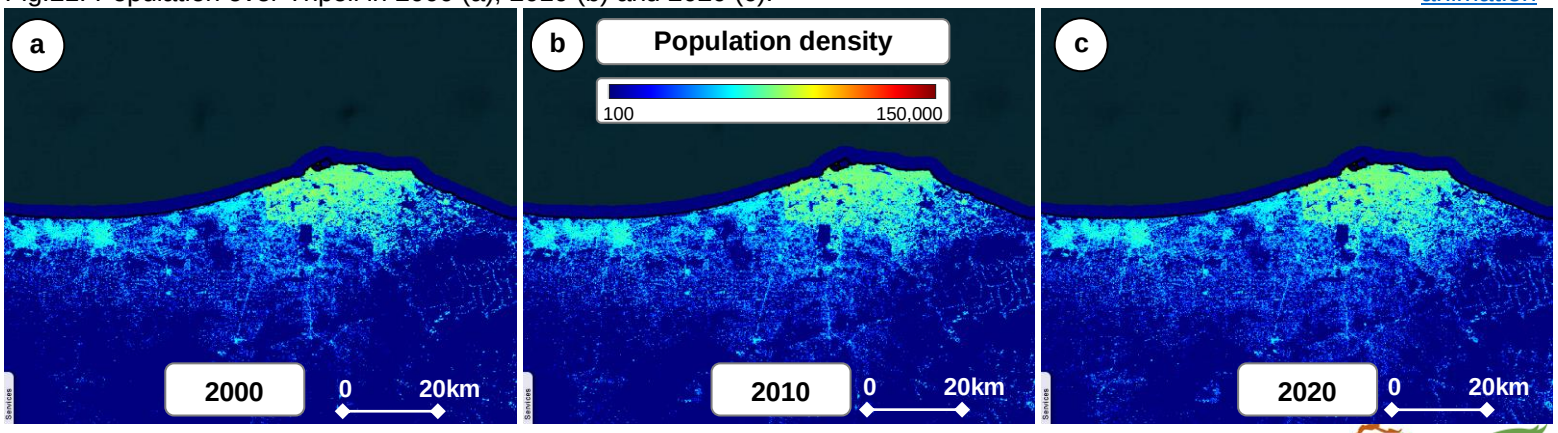

powered by AfEOS and VisioTerra

Deforestation monitoring

Al Beida

Urbanization in northern Libya has led to deforestation, resulting in the decreasing of green cover and the transformation into urban spaces.

Fig.22 shows Sentinel-1 radar views (Fig.a to d) alongside their optical counterparts in Sentinel-2 optical views (Fig.e to h) near the city of El Baida in northeaster Libya. These images are observed in 2018 up to a recent observation on 14 July 2023.

The advantage of radar images is that they penetrate clouds.

This deforestation corresponds to the establishment of a cemetery, expanding over time as depicted in VHR images (Fig.23).

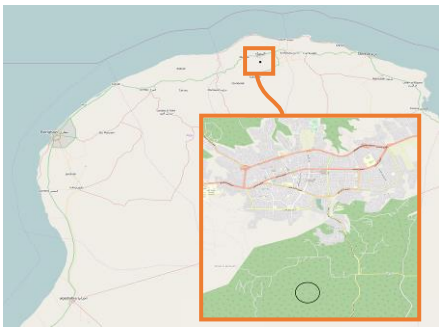

Fig.22: Sentinel-1 and Sentinel-2 views of the evolution of a deforestation observed near to Albeida. S1_animation S2_animation

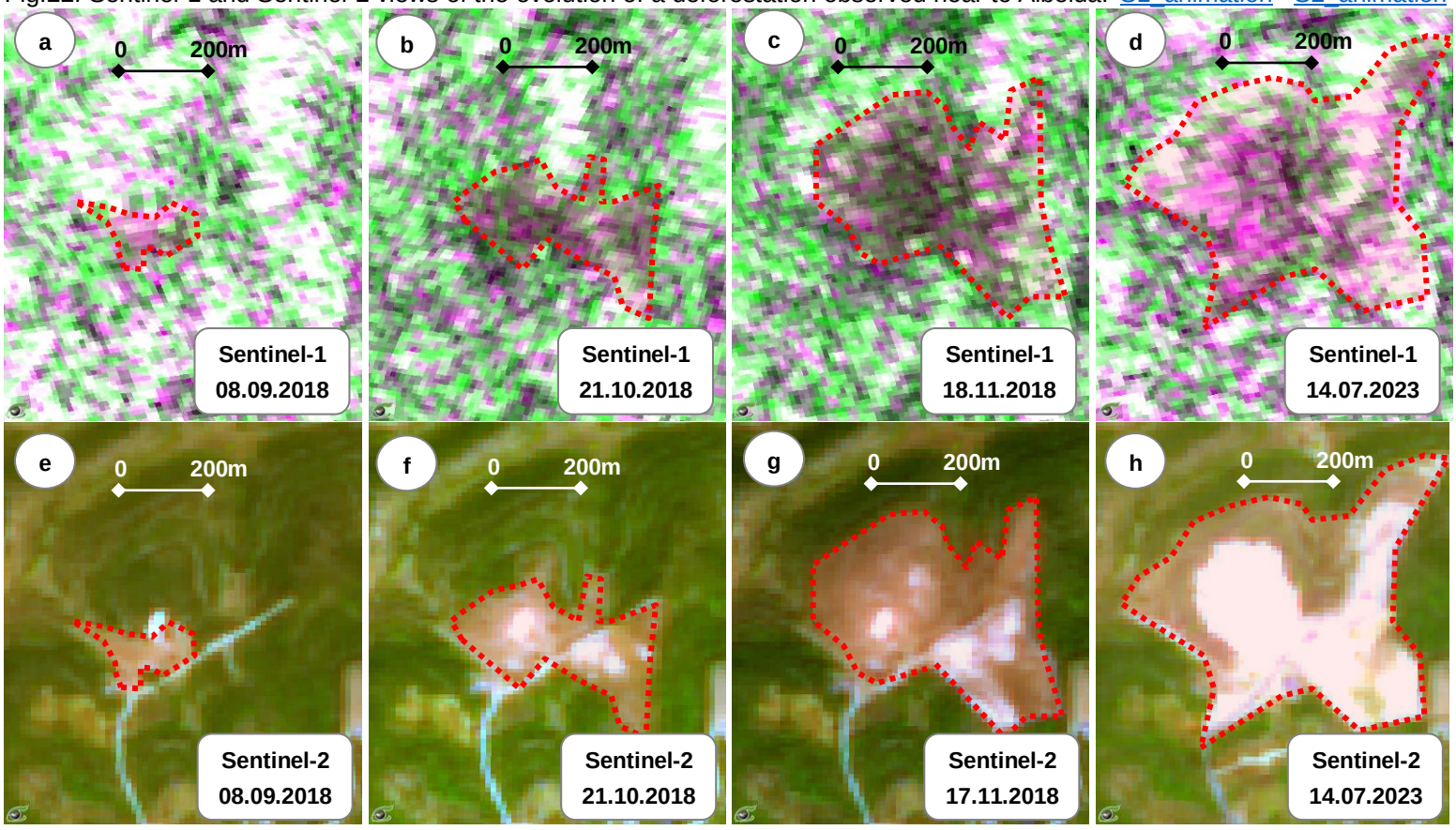

Fig.23: VHR images acquired in 2018 (a) and 2023 (b) showing the establishment of a cemetery.

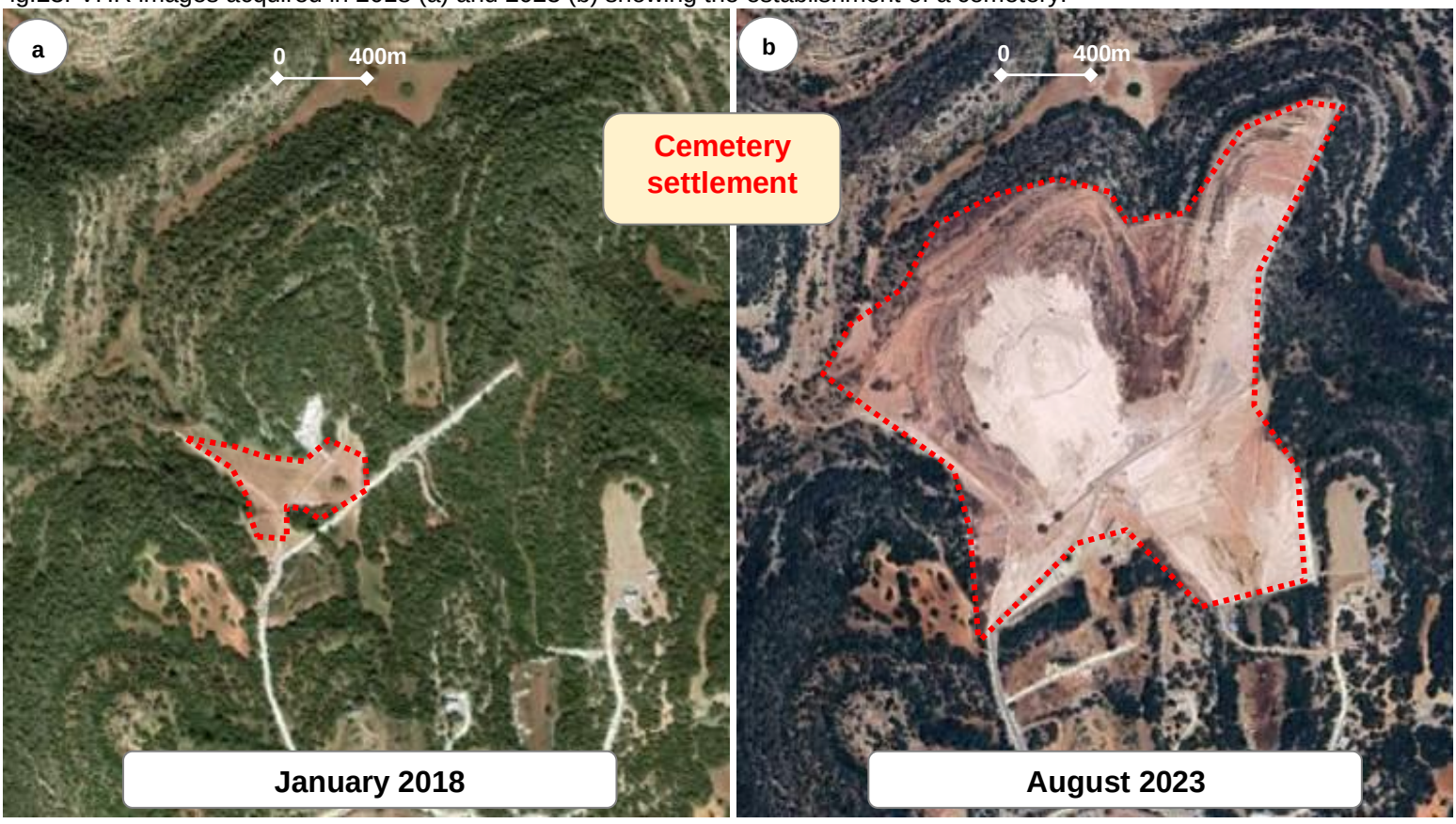

In Libya, floods are infrequent but can be devastating. An example is the floods that occurred in Derna in September 2023 following the passage of Hurricane Daniel. The destruction of a dam resulted in heavy loss of life and widespread devastation.

VisioTerra has implemented flood indicators calculated from Sentinel-1 radar data using Machine Learning methods based on a large number of learning plots. This methodology consists of two steps:

1. Separate the "Water" class from the other land cover classes (bare soil, low vegetation, high vegetation, savannah, built-up area...) detectable from Sentinel-1 radar data.
2. Detect the "Flood" change class, which corresponds to areas that are not usually covered by water but have been invaded by water at some point due to precipitation. Flood recurrence measures the probability of flooding.

The final product is a **flood hazard map**.

Fig.24 and Fig.25 below show Sentinel-1 and Sentinel-2 views before and after Daniel brought a heavy downpour to the region. Sentinel-1 radar images are acquired every 12 days (for a single satellite) or every 6 days (for the constellation of two Sentinel-1 satellites). Since the radar signal passes through the clouds, the regularity of these observations is guaranteed. For each new image (Fig.25b), the difference between the pixels classified as "water" and those of the previous image (Fig.25a) is calculated. This difference produces an additional occurrence of the "flood" class (Fig.26).

Flooding risk monitoring

Derna

Derna, typically safeguarded by dams along the Wadi Derna, suffered severe damage during heavy rainfall. CNN's Nadeen Ebrahim reported the destruction caused by a 7-meter wave, wiping out buildings and infrastructure in the city center, affecting its population of around 100,000.

Fig.24: View Sentinel-2 of north-east Libya before and after Daniel storm brought a heavy downpour to the region. animation

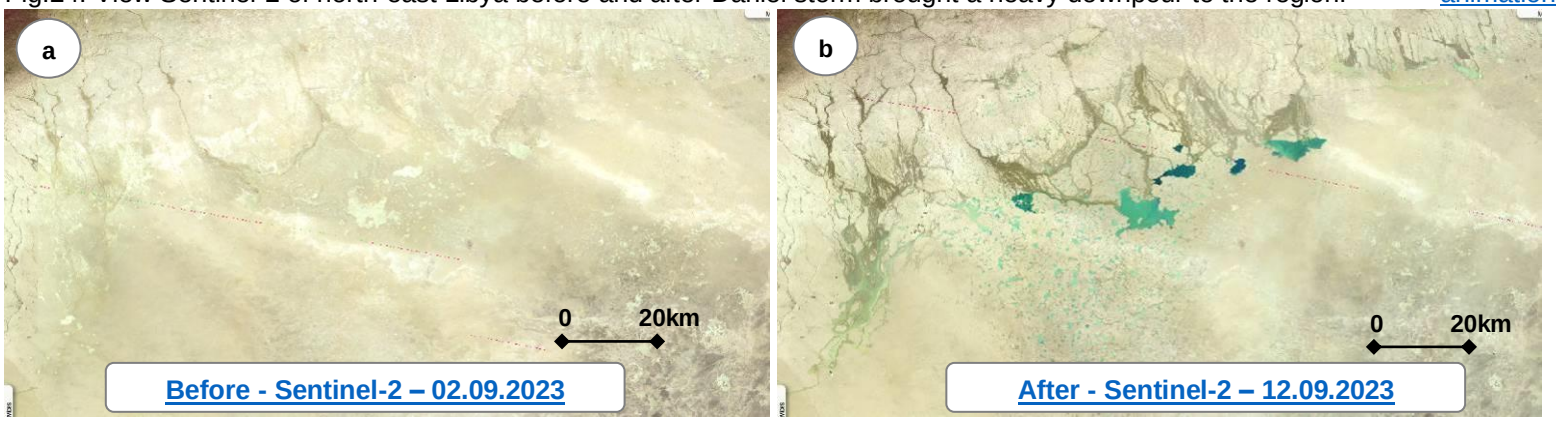

Fig.25: View Sentinel-1 of north-east Libya before and after flooding. animation

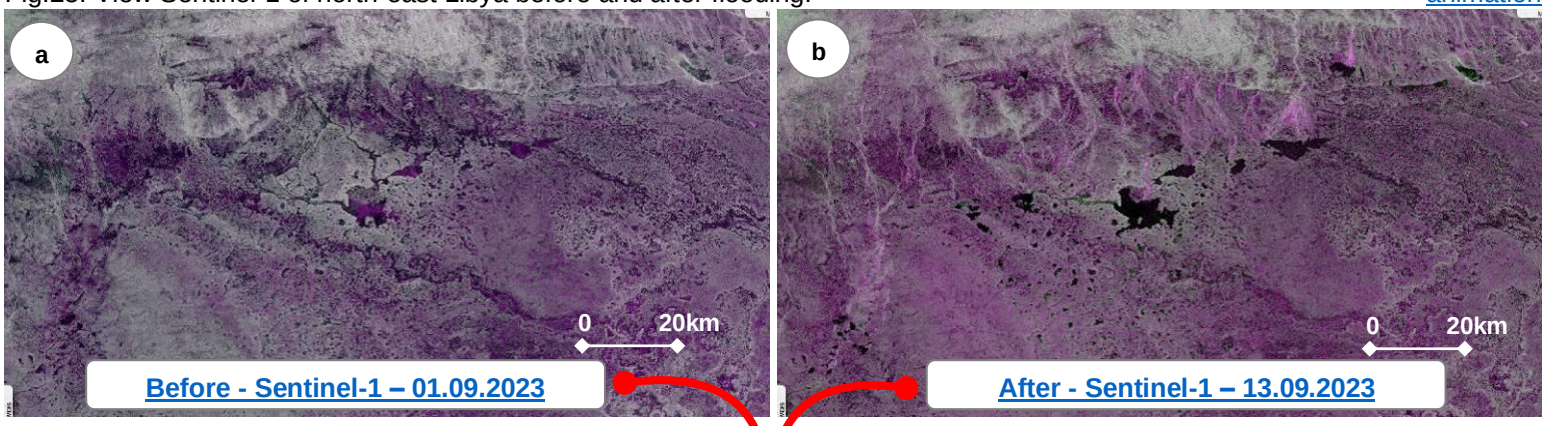

Fig.26: Flooded areas (red).

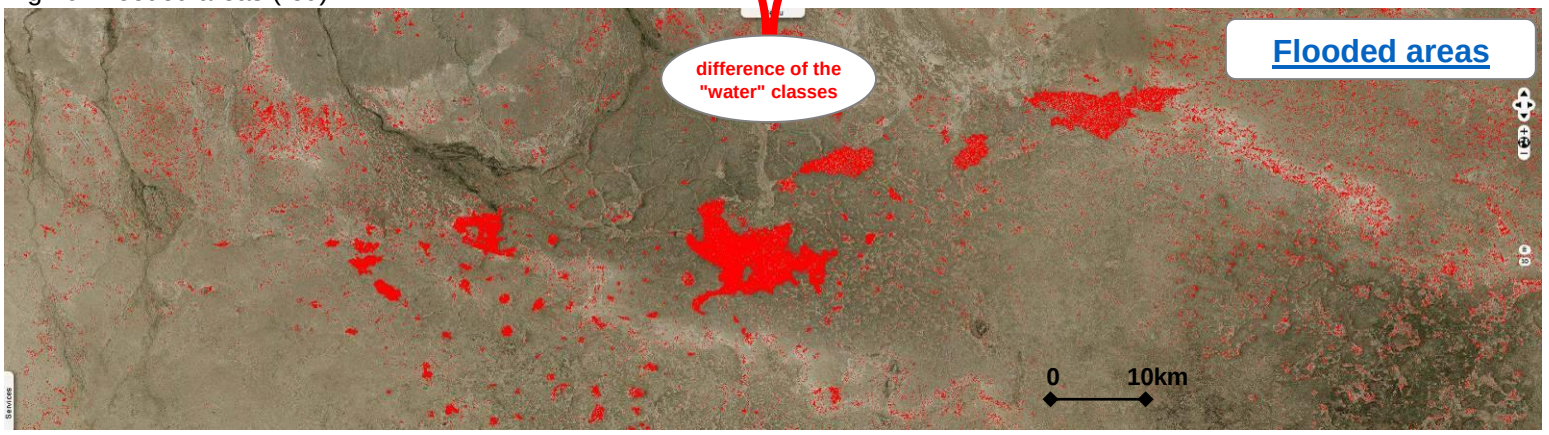

Fig.27: Flooded areas (red) overlaid on Copernicus DEM.

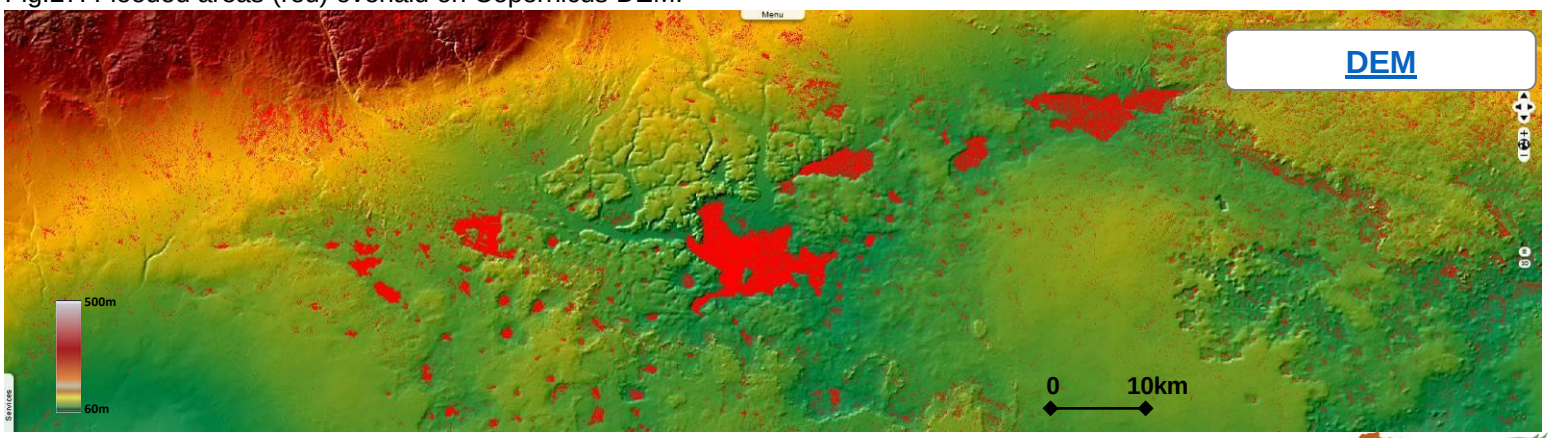

powered by AfEOS and VisioTerra

Offshore oil slicks monitoring

Sentinel-1 radar scenes are useful for monitoring oil slicks in marine areas. The VV polarisation of Sentinel-1 images makes it easy to observe oil slicks on the surface of the sea. These slicks can be witnesses of anthropogenic pollution (Oil spills) caused by the deballasting of ships or leaks from oil platforms. Oil slicks can also have a natural origin from underwater reservoirs (oil seepages).

This section shows a study of oil slicks detected from Sentinel 1 radar images in the Exclusive Economic Zone (EEZ) of Libya.

Fig.28 shows examples of oil spills supposed to come from Farwa FPSO (Floating Production Storage and Offloading) observed on Sentinel-1 radar image acquired on 11 October 2021 and on Sentinel-2 optical image acquired on 9 October 2021 in the EEZ of Libya.

Farwa FPSO platform moored 86 km offshore the Libyan-Tunisian border. It is operated by the Libyan National Oil Corporation (NOC).

The oil spills seem to endanger the Farwah Lagoon marine protected area.

Fig.29 shows an example of likely natural oil seep (Fig.29a) and an example oil spill coming from ship.

Fig.28: Oil spills emanating from the Farwah FPSO. view a view b

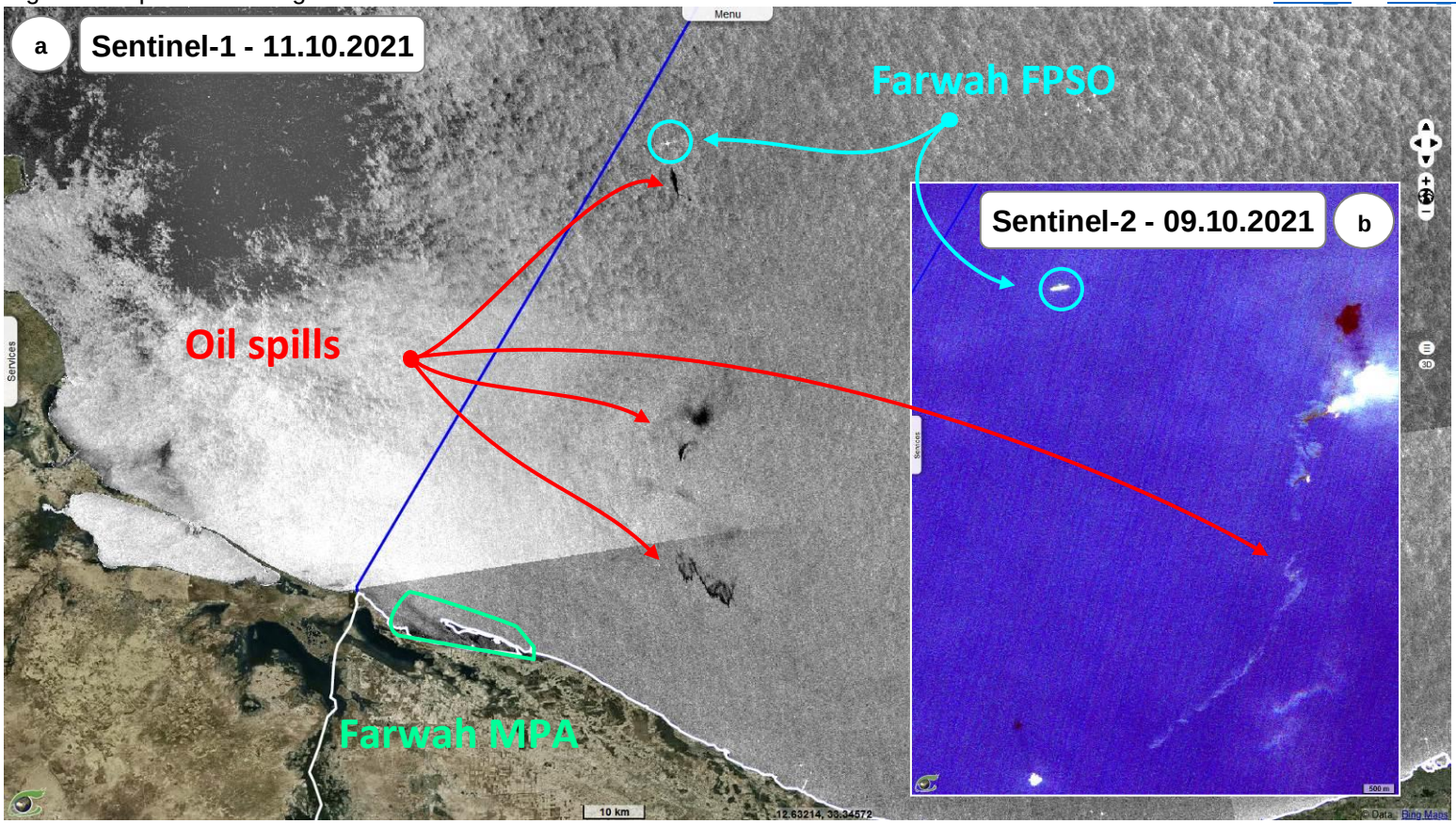

Fig.29: Likely oil seeps (a) and oil spill from ship (b) observed on Sentinel-1 radar images in the Libya EEZ.

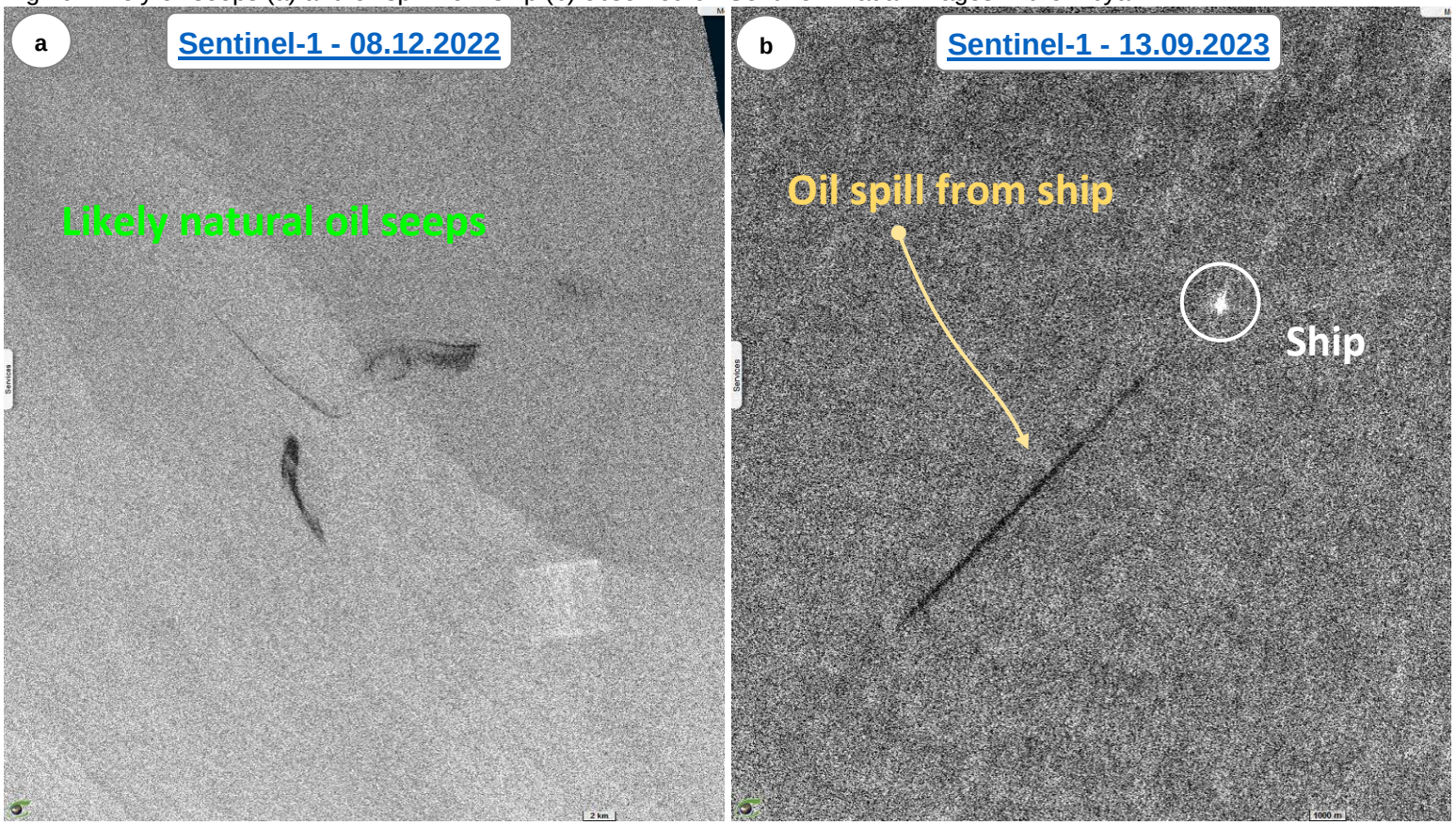

The data of the 6th phase CMIP6 of comparison of the global climate models (CMIP6, 2021) describe the evolution of the essential climate variables among which are the values of temperature MIN (night), temperature MAX (Day) and precipitation according to the two scenarios SSP245 and SSP585 from the 1950s to 2100s. Compared to the radiative forcing of human origin (RCP or Representative Concentration Pathway) implemented in the 5th phase CMIP5 (Coupled Model Intercomparison Project), the 6th phase CMIP6 considers two variables: the reference socio-economic scenarios SP1, SP2, SP3, SP4 and SP5 (considering GDP per capita, population, governance, education and technology) and radiative forcing of 2.6, 4.5, 6.0 and 8.5 W/m² as in the CMIP5 project. This combination appears in the SSP (Shared Socioeconomic Pathways) scenario name. For example, SSP245 corresponds to SSP2 at 4.5 W/m² and SSP585 corresponds to SSP5 at 8.5 W/m². In this study, the data used come from the IPSL model.

See https://visioterra.fr/web/Climate-change?lang=en

Fig.30 show the evolution of the three variables: -MIN temperature (nighttime, Tmin), -MAX temperature (daytime, Tmax) and precipitations (Pr) according to the two scenarios SSP245 and SSP585 for the years 2000, 2020, 2040, 2060, 2080 and 2100. Fig 31 show a differential analysis carried out in relation to the reference year (2000).

Climate change
Tmin, Tmax, Pr

The results of this analysis show an increase in maximum and minimum temperatures for the two scenarios for the whole Libya. Meanwhile, the precipitation is decreasing.

Fig.30: Evolution of Tmin and Tmax and Pr in Libya. T_{min} (SSP245 and SSP585) +T_{max} (SSP245 and SSP585)+ Pr (SSP245 et SSP585)

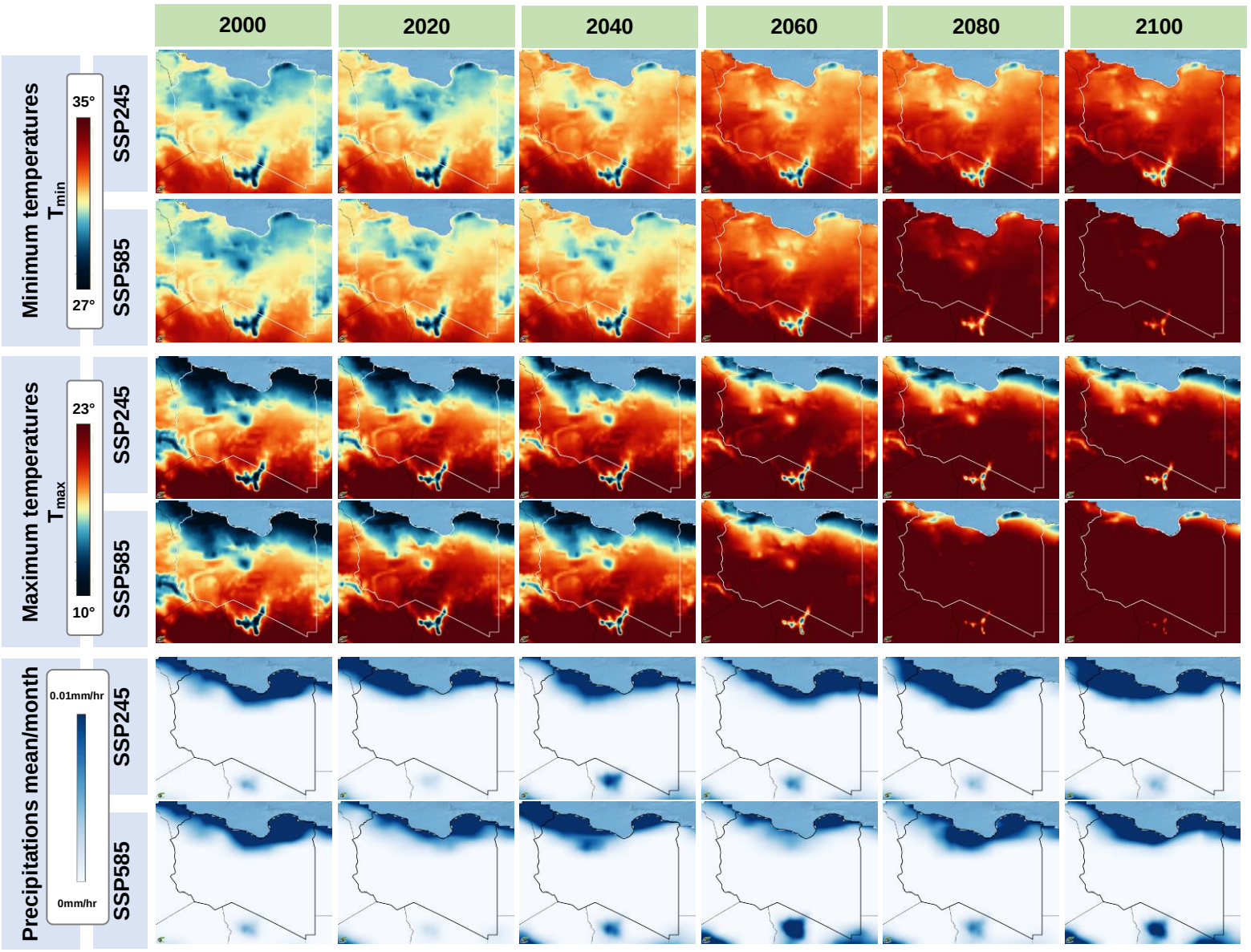

Fig.31: Differential analysis in relation to the reference year (2000) for Tmin, Tmax and precipitations for the two scenarios.